

Giant Resonances

Stanley S. Hanna

Department of Physics, Stanford University, Stanford,
California 94305, U.S.A.*

Abstract

A review is given of giant multipole resonances in nuclei with emphasis on their systematic location, their great strength in terms of an appropriate sum rule and their concentration in a rather narrow region. Capture reactions as a source of information are especially considered.

1. Introduction

In recent years there has been a resurgence of interest in the giant multipole resonances. This interest has been stimulated by the location of resonances in the heavier nuclei and by the advent of new ways of studying them. Thus, in addition to the older methods of electron or γ -ray scattering and absorption, and inverse capture reactions, the inelastic excitation by hadronic particles is now being used extensively to observe the different multipole resonances, especially in heavy nuclei. The processes involving γ -ray excitation selectively excite the electric and magnetic dipole states and to a lesser degree the quadrupole strength. The inelastic excitations, both electronic and hadronic, have the advantage of exciting all multipoles more or less equally, depending on the momentum transfer, but are subject to the difficulties of sorting out the various multipoles from each other and from the large backgrounds of generally mixed multipolarity. However, a careful choice of experimental conditions greatly facilitates the identification and study of the various resonances.

In this paper I stress the three basic properties of a 'giant' resonance: its systematic location in all nuclei, its great strength in terms of an appropriate sum rule, and its concentration in a rather narrow region. I begin with a brief review of these properties for the giant E1 resonance, which are now well established. I then discuss the recent advances in our knowledge of the E1 resonance which have come from the polarized proton capture measurements. I then survey and discuss the existing knowledge on M1 resonances and E2 strengths, both isoscalar and isovector, with emphasis on the information obtained from capture reactions.

2. Basic Properties of Giant E1 Resonance

The giant electric dipole (E1) resonance has long been the object of intensive study. The three important properties which characterize it are its systematic occurrence in all nuclei, its great strength, and its localized nature (Fuller *et al.* 1973).

* Supported in part by the U.S. National Science Foundation.

(1) In the medium and heavy nuclei the E1 resonance occurs at an energy of $77 A^{-1/3}$ MeV. However, in the light nuclei, below ^{40}Ca , the energy of the resonance falls off as shown by the continuous curve in Fig. 1. We note here that, if the giant E2 resonance maintains a position of $63 A^{-1/3}$ MeV in the light nuclei then the E2 resonance (dashed line in Fig. 1) will cross the E1 resonance and lie above it in the lightest nuclei.

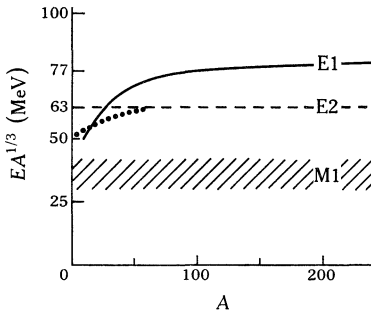


Fig. 1. Location in energy E of the giant E1, E2 and M1 resonances as a function of the mass number A . (See text for a discussion of the M1 and E2 behaviour.)

(2) The giant E1 resonance 'exhausts' the classical E1 sum rule $60 NZA^{-1/3}$ mb MeV. Actually it is now known that the total strength exceeds this sum rule and this has been the object of recent study. However, this phenomenon will not concern us here.

(3) Perhaps the most impressive feature of the E1 resonance is its localized nature, despite the fact that it occurs in the continuum where many decay channels are open. From the lightest to the heaviest nuclei the width is given by $\Gamma/E \approx 1/5$, with several notable exceptions which can be attributed to the following causes:

- (i) nuclear deformation (well established),
- (ii) isospin splitting (well established in certain nuclei),
- (iii) excitation of deep hole states (not yet well established).

There are many other interesting and significant properties of the E1 resonance which are not discussed here (see Hanna 1969*a*). Instead, we turn to the new information which has been obtained on the configurations of the E1 resonances from the polarized proton beam (p, γ) reaction.

3. Configurations of E1 Resonance

The particle-hole model has quite successfully described many of the dominant features of the giant E1 resonance (GDR) in nuclei, and in its simplest form provides naturally for the characteristic single-particle transitions of the type $l_j \rightarrow (l+1)_{j+1}$ (no spin flip) which carry large E1 strengths (Wilkinson 1959). However, in the region of the GDR, finer structure in the total cross section is often observed in capture reactions such as (p, γ_0) and in the inverse photonuclear reactions. A question that immediately arises is whether or not this structure is indicative of a change in nuclear configuration as one passes through the GDR, as has often been suggested. Not only have changes in the $(1p-1h)$ configurations been proposed, but $(2p-2h)$ or $(3p-3h)$ configurations have also been invoked to explain the observed structure. In both light nuclei such as ^4He (Meyerhof *et al.* 1970) and heavy nuclei such as ^{142}Nd (Hasinoff *et al.* 1972), spin-flip transitions have also been assigned an important role in GDR.

In contrast to the idea of a changing configuration is the remarkable constancy of the angular distributions observed throughout the GDR (Allas *et al.* 1964*b*), including such well-defined levels as the analogue states (Hasinoff *et al.* 1969) which are often assigned to configurations different from the GDR. To improve our understanding of the configurations in a GDR, it is very helpful to know the relative phases as well as the amplitudes of the reaction matrix elements associated with the channels which form a GDR. For the proton channel, for example, these can be found only by combining angular distribution measurements made on the polarized reaction (p, γ_0) with unpolarized angular distribution data. As is seen below, in many cases, unique solutions for the reaction amplitudes are obtained from such measurements.

We define a complete experiment as one in which the cross section is determined as a function of all physical parameters and, for the (p_0, γ_0) channel of the GDR, we write the cross section as

$$\sigma(E_\gamma, \theta_\gamma, P_p, P_\gamma),$$

where E_γ is the excitation energy in the GDR, θ_γ is the angle between p and γ , P_p is the proton polarization and P_γ is the γ -ray polarization. Extensive angular distribution measurements on many nuclei (Allas *et al.* 1964*b*) have shown that the radiation is predominantly dipole, with small admixtures of dipole-quadrupole radiation of opposite parity. Thus, we have for the multipolarity of the radiation either

$$E1 \text{ mixed with } (M1, E2) \quad \text{or} \quad M1 \text{ mixed with } (E1, M2).$$

Because of the great strength of the resonance the first choice has been universally assumed. Hence, we eliminate P_γ from consideration, and the 'complete' cross section becomes

$$\sigma(E_\gamma, \theta_\gamma, P_p).$$

We consider first the unpolarized experiment. It is well known that the cross section can be expanded as follows

$$\sigma(E, \theta) = A_0(E) \left(1 + \sum_{k=1}^4 a_k(E) P_k(\theta) \right), \quad (1)$$

where $A_0(E)$ gives the resonance strength. The relationship between the a_k and the multipolarity of the radiation is given in the following tabulation:

| Radiation | E1 or M1 | E2 | (E1, M1) | (E1, E2) | (M1, E2) |
|------------------------------------|----------|------------|----------|------------|----------|
| Unpolarized $\sigma(E, \theta)$ | a_2 | a_2, a_4 | a_1 | a_1, a_3 | a_2 |
| Polarized $\mathcal{A}(E, \theta)$ | b_2 | b_2, b_4 | b_1 | b_1, b_3 | b_2 |

In all cases that have been investigated, the M1 and E2 contribution may be important in $a_1(E)$ and $a_3(E)$, but can be neglected in $a_2(E)$ and $a_4(E)$. Thus we may extract from the data

$$\sigma(E, \theta) = A_0(E) \{ 1 + a_2(E) P_2(\theta) \}, \quad (2)$$

where $A_0(E)$ and $a_2(E)$ carry the information on the E1 resonance in the (p, γ) reaction.

We now consider the polarized experiment, in which the γ -ray yield is sensitive to the degree of polarization perpendicular to the reaction plane. It is convenient to

measure the analysing power

$$\mathcal{A}(E, \theta) = (\sigma_{\uparrow} - \sigma_{\downarrow}) / (\sigma_{\uparrow} + \sigma_{\downarrow}), \quad (3)$$

where σ_{\uparrow} and σ_{\downarrow} are the γ -ray yields, with p spin up and down respectively, normalized to a 100% polarized beam.

The analysing power can be expanded as follows:

$$\mathcal{A}(E, \theta) \sigma(E, \theta) = A_0(E) \left(\sum_{k=1}^4 b_k(E) P_k^1(\theta) \right), \quad (4)$$

where the relationship between the coefficients b_k and the multipolarity of the radiation is as given in the above tabulation. Again, if we are interested in the E1 strength, we may neglect the M1 and E2 contribution to b_2 and extract from the polarization measurements

$$\mathcal{A}(E, \theta) \sigma(E, \theta) = A_0(E) b_2(E) P_2^1(\theta), \quad (5)$$

where $b_2(E)$ carries the information on the E1 resonance. Thus, in the complete experiment we obtain the three quantities

$$A_0(E), \quad a_2(E) \quad \text{and} \quad b_2(E)$$

measured over the E1 giant resonance. We may now pass from these three quantities to the configurations in the proton channel of the GDR. The proton configurations can, of course, be expressed in any desired coupling scheme. We may indicate this transformation formally by

$$\begin{bmatrix} A_0(E) \\ a_2(E) \\ b_2(E) \end{bmatrix} \rightarrow \begin{bmatrix} \text{proton configuration} \\ \text{in } jj, LS \text{ or other} \\ \text{coupling scheme} \end{bmatrix}. \quad (6)$$

Some illustrations of this transformation are given in the following examples. Finally, we must relate the configuration of the proton channel to the giant resonance itself. This is the task of theory, but it is clear that the observed proton configurations will severely restrict the allowed configurations of the GDR. A theoretical treatment of ^{16}O is given in subsection (b) below.

(a) E1 Resonance in ^{16}O

In Figs 2a-2d are shown respectively the data for $A_0(E)$, $a_1(E)$, $a_2(E)$ and $a_3(E)$ taken from the unpolarized experiment of Black *et al.* (1967) and O'Connell (1969). These data were obtained from detailed angular distribution measurements. It can be seen in Fig. 2 that the coefficients a_1 and a_3 indicate the presence of E2 and possibly M1 radiation, but we now confine our attention to A_0 and a_2 , as discussed above. It is seen that $a_2(E)$ is quite constant over the resonance at the 'dipole value' of -0.6 except in two regions where there is also marked fine structure in the total cross section $A_0(E)$.

It has been remarked (Gillet *et al.* 1967) that this structure in A_0 correlates well with resonances seen in the (d, γ), (^3He , γ) and (α , γ) reactions which might indicate (n -particle, n -hole) configurations in ^{16}O . It is in fact possible to decompose the GDR

into basic states (presumably the predicted $1p-1h$ states) and three sharper states (presumably $np-nh$ states) which interfere in a characteristic manner with the two basic states (see Black *et al.* 1967; O'Connell 1969). Also, Shakin and Wang (1971) and Wang and Shakin (1973) have obtained agreement with the structure in A_0 using only $3p-3h$ states. This is an attractive picture and, although not firmly established, we adopt it in our discussion.

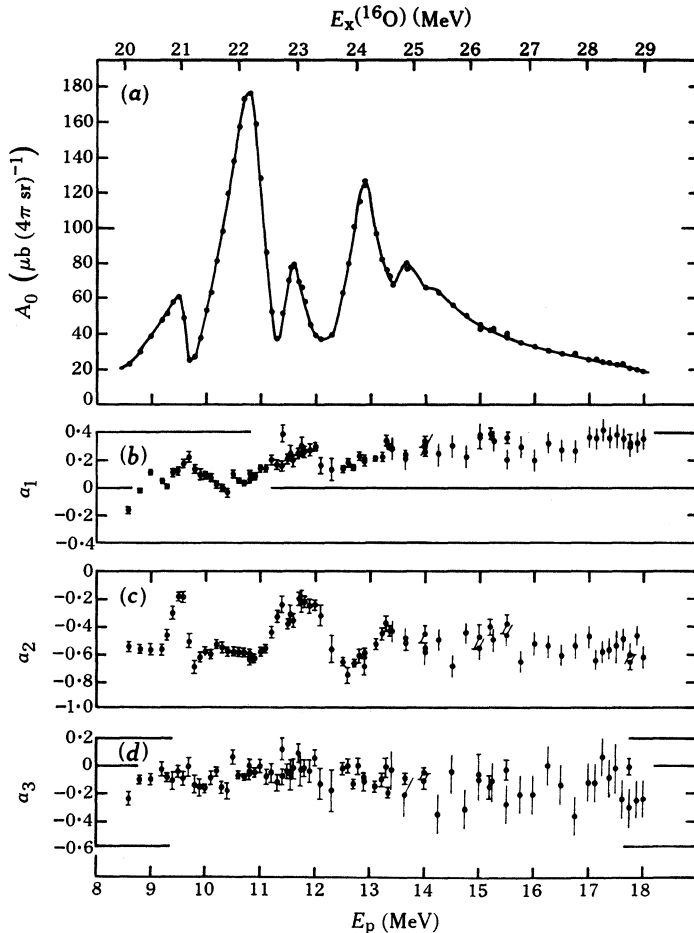


Fig. 2. Total yield A_0 and angular distribution coefficients a_1 , a_2 and a_3 in $^{15}\text{N}(p, \gamma)^{16}\text{O}$ (O'Connell *et al.* 1973).

We now pass from the quantities A_0 and a_2 to the amplitudes of the proton channel in jj representation (in conformity with the transformation (6) above) in the reaction $^{15}\text{N}(p, \gamma)^{16}\text{O}$. Only incident proton waves with $(l = 0, j = 1/2)$ and $(l = 2, j = 3/2)$ can combine with the $1/2^-$ ground state of ^{15}N to form a 1^- state in ^{16}O . Thus for E1 radiation we have the transition scheme $1/2^-(s_{1/2}, d_{3/2})1^-(\text{E1})0^+$ which determines the angular distribution. The corresponding matrix elements may be written as

$$|s_{1/2}| \exp(i\phi_s) \quad \text{and} \quad |d_{3/2}| \exp(i\phi_d),$$

where $s_{1/2}$ and $d_{3/2}$ are the real amplitudes and ϕ_s and ϕ_d the real phases. From a

straightforward calculation we obtain

$$a_2 = -0.5 d_{3/2}^2 + \sqrt{2} |s_{1/2}| |d_{3/2}| \cos(\phi_d - \phi_s), \quad (7)$$

$$1 = s_{1/2}^2 + d_{3/2}^2. \quad (8)$$

The normalization (8) eliminates A_0 from further consideration.

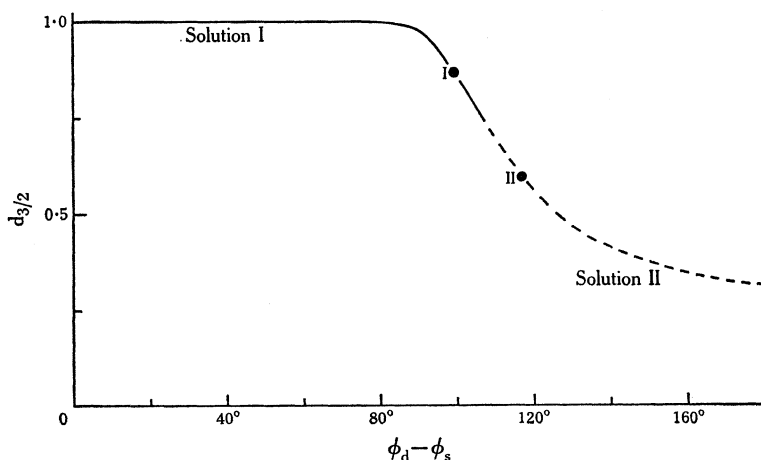


Fig. 3. Allowed solutions (I and II) for the p_0 channel of $^{16}\text{O}(\gamma, p_0)^{15}\text{N}$. The curves give the values of $d_{3/2}^2$, $s_{1/2}^2$ and $\cos(\phi_s - \phi_d)$ allowed by $a_2 = -0.48$, while the dots are the unique solutions produced by the additional condition $b_2 = 0.3$.

We can now appreciate the problem of having only unpolarized results available: there are three unknown quantities, namely $s_{1/2}$, $d_{3/2}$ and $\phi_d - \phi_s$, but only two relationships (7) and (8) to determine them. Of course, the experimental value of a_2 severely restricts the amplitudes and phases but does not uniquely determine them. It is possible to plot the allowed solutions as curves in amplitude-phase space as done in Fig. 3. Since the expressions (7) and (8) are quadratic there are two equally acceptable solutions which are labelled I (solid curve) and II (dashed curve) in Fig. 3. The solutions are shown for $a_2 = -0.5$, which is representative of the value throughout the whole GDR, except for the regions where there is fine structure. We note that there is one solution (I) which is predominantly d wave while the other (II) is predominantly s wave. The simple particle-hole model would of course prefer the former solution.

We now turn to the polarized measurements on $^{15}\text{N}(p, \gamma)^{16}\text{O}$ carried out at Stanford University, to see what light they can shed on the configurations in ^{16}O . If the analysing power is measured as a function of angle at each energy then the quantity $b_2(E)$ can be obtained from equation (5). This new quantity can then be expressed in terms of the amplitudes and phases

$$b_2 = \frac{1}{2}\sqrt{2} |s_{1/2}| |d_{3/2}| \sin(\phi_d - \phi_s), \quad (9)$$

which gives a third relationship to go with (7) and (8). Thus, we have three equations and three unknowns, and unique solutions (I and II) can be obtained.

The measurements were carried out with a polarized beam provided by a polarized ion source of the atomic-beam sextupole magnet type (Glavish 1971) and accelerated by the Stanford FN tandem Van de Graaff. The beam currents at the target were about 10 nA. The ^{15}N target consisted of ^{15}N gas (>90%) at 200 torr in a gas cell 5 cm long. The γ rays from the reaction were detected with the Stanford 24×24 cm NaI spectrometer (Suffert *et al.* 1968). To minimize the background, the cell was

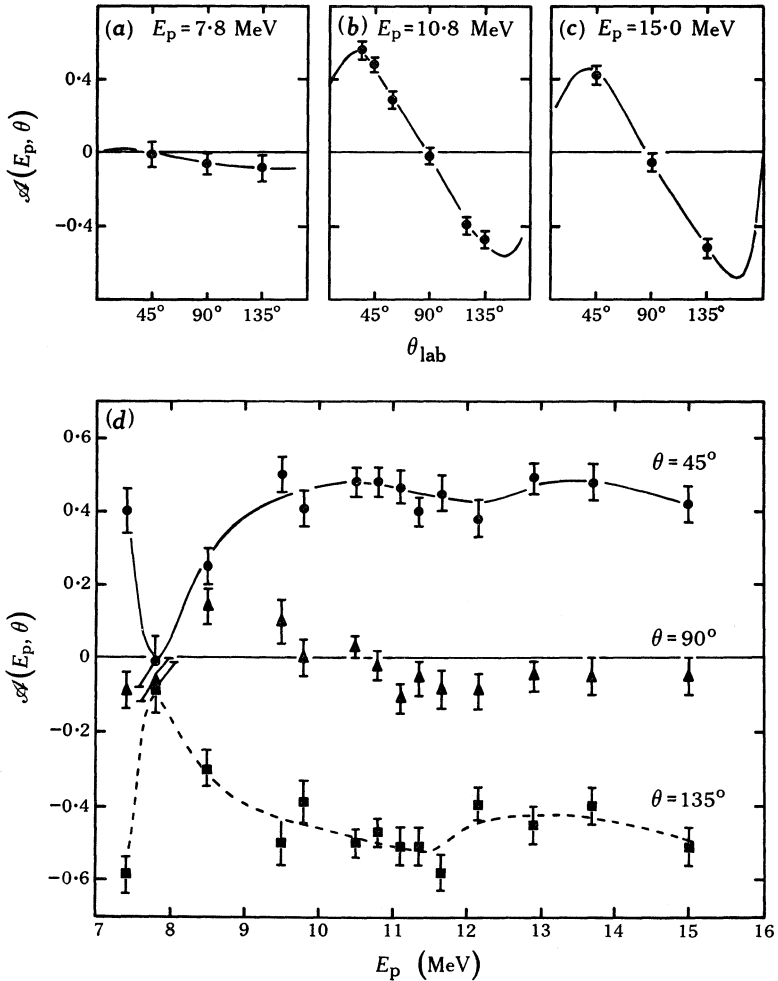


Fig. 4. Measured analysing powers $\mathcal{A}(E_p, \theta)$ for $^{15}\text{N}(p, \gamma_0)^{16}\text{O}$, showing (a)–(c) $\mathcal{A}(\theta)$ for three selected energies; and (d) $\mathcal{A}(E_p)$ for three selected angles.

equipped with an exit window in addition to the entrance window. After passing through the cell the beam was stopped 7 m downstream behind concrete shielding.

The spin direction for the protons could be set either up or down by selecting the appropriate RF transition in the polarized ion source. At a given energy and angle, the analysing power $\mathcal{A}(E, \theta)$ defined by equation (3) was determined from measurements made by frequently alternating runs with proton spin up and runs with proton spin down. Several times during the experiment the proton polarization was measured

by observing the asymmetry in elastic scattering from ^{12}C at $E_p = 9.8$ MeV and $\theta_{\text{lab}} = 70^\circ$, where the analysing power for ^{12}C is well known (Moss and Haeberli 1965). The proton polarization was typically 0.5, and varied by only a small amount over long periods of time.

A fairly complete survey of the GDR in ^{16}O was made by measuring $\mathcal{A}(E, \theta)$ at laboratory angles of 45° , 90° and 135° , at 14 energies ranging from 7.4 to 15.0 MeV. The results are shown in Fig. 4. Many of the energies were selected to coincide with the peaks and valleys of the structure exhibited in the total cross section of the reaction $^{15}\text{N}(p, \gamma_0)^{16}\text{O}$ (see Fig. 2). Results for the small resonances (Earle and Tanner 1967) at $E_p = 7.4$ and 7.8 MeV below the main part of the GDR are also included in Fig. 4.

The results in Fig. 4 show that, throughout the GDR ($E_p > 9$ MeV), $\mathcal{A}(\theta)$ has a pronounced $P_2^1(\theta)$ or $\sin 2\theta$ dependence which is consistent with predominant dipole radiation. Measurements of $\mathcal{A}(\theta)$ at just the three angles 45° , 90° and 135° are sufficient to determine the coefficient b_2 and to establish that b_1 and b_3 are small by comparison. For instance, at $E_p = 10.8$ MeV the curve drawn through the experimental points corresponds to the values $b_1 = 0$, $b_2 = 0.26$ and $b_3 = 0.02$. At each energy the coefficient b_2 was determined from the measured value of $\mathcal{A}(\theta)$ and $\sigma(\theta)/A_0$ as obtained from the coefficients a_1 and a_2 given by Black *et al.* (1967) and O'Connell (1969) (see equation 5). The values obtained for b_2 are shown in Fig. 5d along with the curves for A_0 , a_1 and a_2 in Figs 5a–5c.

Throughout the main part of the GDR we see that b_2 is fairly constant at a value of about 0.3. The constancy of both a_2 and b_2 means that the configuration in the proton channel remains constant throughout the GDR no matter what is happening to the configuration of the GDR itself. This is a very remarkable result.

If we now impose the added condition (9) and adopt $b_2 = 0.3$ as representative of the entire GDR we obtain the unique solutions I and II corresponding to the solid circles shown in Fig. 3. These are the characteristic solutions of the proton channel of the GDR.

It is of course interesting to see what causes the fluctuations in the coefficient a_2 . This can be determined by obtaining the solutions at each experimental point. These solutions are shown in Figs 5e and 5f. As we saw in Fig. 3, solution I (solid curve) is characterized by a dominant $d_{3/2}$ capture with an average value for $d_{3/2}^2$ of about 0.90. Solution II (dashed curve) corresponds mainly to $s_{1/2}$ capture with an average value for $s_{1/2}^2$ of about 0.80. However, the remarkable feature of both solutions is the constancy of the $s_{1/2}$ and $d_{3/2}$ amplitudes throughout the entire structure of the GDR.

The structures in the total cross section of ^{16}O at excitations of 21 and 23 MeV are both characterized by large rapid variations in the value of a_2 , as noted above. The polarization results show that this behaviour arises almost entirely from fluctuations in the phase difference $\phi_d - \phi_s$ rather than in the $s_{1/2}$ and $d_{3/2}$ amplitudes, as seen from Figs 5e and 5f.

Only one of the two solutions I and II should be physically correct, the other being just a mathematical solution. Bound state calculations (Gillet and Vinh-Mau 1964) are most consistent with solution I, which has the large d-wave amplitude. In trying to decide experimentally which of the two solutions is physically correct it is interesting to compare the polarization effects in $^{15}\text{N}(p, \gamma_0)^{16}\text{O}$ with those in $^{16}\text{O}(\gamma, n_0)^{15}\text{O}$ (Bertozzi *et al.* 1964; Nath *et al.* 1973). At an angle of 45° , the measured values for the neutron polarization are slightly smaller than the values obtained for the proton polarization. To the extent that charge independence is valid, the two proton solutions

can be adjusted to apply to neutrons by taking into account the difference in proton and neutron penetrabilities and removing the Coulomb phase of the protons. We then find that solution I predicts a neutron polarization consistent with the experimental data, while solution II leads to a much smaller value.

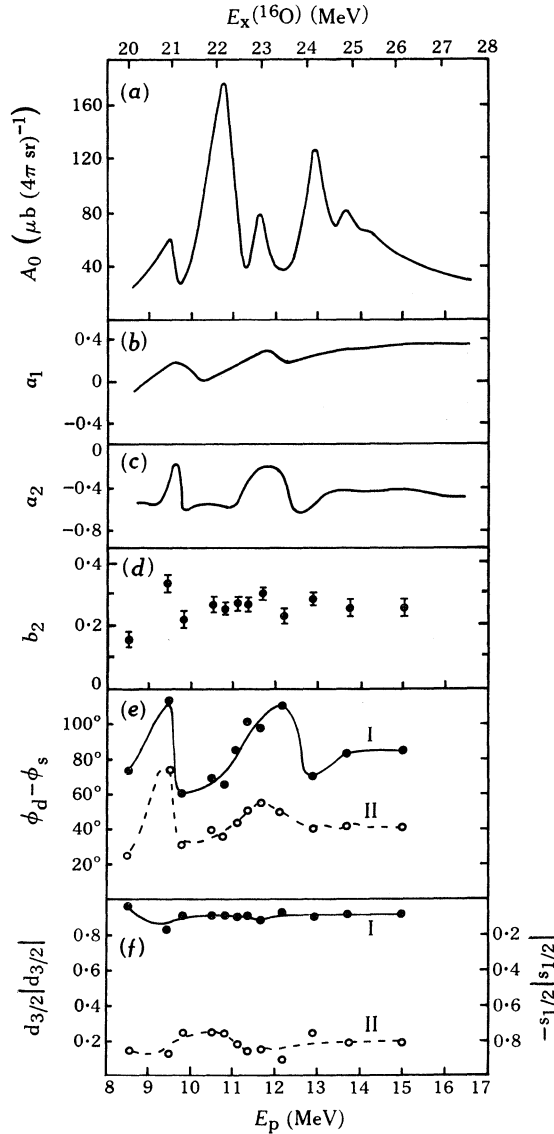


Fig. 5. Summary of E1 information on the GDR in $^{15}\text{N}(p, \gamma_0)^{16}\text{O}$. The two solutions for the proton channel are indicated by I and II.

The polarization effect for the reaction $^{15}\text{N}(p, \gamma_0)^{16}\text{O}$ becomes very small at the resonance at $E_p = 7.8$ MeV just below the main GDR and then returns to a 'normal' value at the next lower resonance at $E_p = 7.4$ MeV (see Fig. 4). If the 7.8 MeV resonance is a 1^- state, as proposed by Earle and Tanner (1967), the large value of a_2 they reported at this resonance would require $\phi_d - \phi_s \approx 0$. This would be an

unusual result when compared with the behaviour at any of the other 1^- structures in the GDR. Another possible assignment for the 7.8 MeV resonance is 1^+ (Barber *et al.* 1963). In this case the interfering proton waves would both be p waves and the matrix elements might be expected to have nearly the same phase, in which case the analysing power would necessarily be zero.

The polarization measurements have shown that in ^{16}O the fluctuations in the dependence of a_2 on energy are caused by fluctuations in the relative phases of the s and d proton channels and not by fluctuations in their amplitudes. It will be interesting to see if refinements in the theories of the GDR in ^{16}O can account for this phenomenon.

(b) *Theory of E1 Resonance in ^{16}O*

As we have seen, the giant dipole resonance of ^{16}O exhibits two dominant peaks (see Fig. 2a) at excitation energies of 22.3 and 24.4 MeV. These two peaks carry a major part of the E1 strength and have been interpreted as collective single particle-hole excitations generated from a particle-hole interaction acting on unperturbed single-particle shell-model excitations (Elliot and Flowers 1957; Brown *et al.* 1961; Gillet and Vinh-Mau 1964). In terms of this model the two peaks are predicted to have quite different particle-hole configurations, being dominantly $d_{5/2}p_{3/2}^{-1}$ at 22.3 MeV and $d_{3/2}p_{3/2}^{-1}$ at 24.4 MeV. On the other hand, we have seen that the angular-distribution and polarization measurements in the $^{15}\text{N}(p, \gamma_0)^{16}\text{O}$ reaction show that the $s_{1/2}$ and $d_{3/2}$ proton capture matrix elements (the only ones allowed for E1 radiation by angular momentum and parity conservation) have remarkably constant relative amplitudes over both peaks. The following calculation was made to see if the simple shell-model description can account for such constancy.

The matrix elements T_{ij} were determined with the formalism of Feshbach *et al.* (1967), which gives (Shakin and Wang 1971; Wang and Shakin 1973)

$$T_{ij} = \langle lj | D_\gamma | 0 \rangle + \sum_k \langle lj | V_{\text{ph}} | d_k \rangle \langle d_k | D_\gamma | 0 \rangle (E - E_k + i\frac{1}{2}\Gamma_k)^{-1}, \quad (10)$$

where $|lj\rangle$ describes the continuum nucleon and the hole state of the mass 15 target nucleus. The doorway states $|d_k\rangle$ are the two collective particle-hole configurations, and E_k and Γ_k are their energies and widths. The particle-hole interaction V_{ph} was taken as

$$V_{ij} = -584 \cdot 1(0 \cdot 865 + 0 \cdot 135 \sigma_i \cdot \sigma_j) \delta(\mathbf{r}_i - \mathbf{r}_j).$$

The quantity D_γ is the electric dipole operator. The unperturbed single-particle wavefunctions were generated from a real Wood-Saxon well, adjusted to reproduce correctly the single-particle energies.

The results of the calculation for the $^{15}\text{N}(p, \gamma_0)^{16}\text{O}$ reaction are compared with the results discussed above (somewhat altered on the basis of new data) in Fig. 6. It is apparent that the calculations are consistent with solution I and are able to reproduce the approximate constancy in the $s_{1/2}$ and $d_{3/2}$ amplitudes. Even the phase difference is quite well reproduced. In Figs 6e and 6f, a comparison is made with the experimental quantities a_2 and b_2 , and it can be seen that the remarkable constancy of these coefficients is quite well reproduced. In fact, the discrepancy in a_2 in the region $E_x = 20$ –22 MeV can be traced to the discrepancy in fitting the relative phase in this region and is therefore probably not a serious matter. The discrepancy in a_2 is amplified because the cosine term is very sensitive to $\theta_d - \theta_s$ when this phase difference is near 90° .

The theoretical curves in Fig. 6 include a small third doorway at $E_x = 19.7$ MeV of predominantly $s_{1/2} p_{3/2}^{-1}$ configuration. Although equation (10) does not show doorway-doorway couplings, these were actually included in the calculations but they did not make a substantial difference to the quality of the fit (full curve in Fig. 6d). The doorway width is the sum of two parts $\Gamma_k = \Gamma_p + \Gamma_Q$, where Γ_p describes the damping to the continuum and can be calculated, while Γ_Q is the damping to more complicated nuclear configurations and is an adjustable parameter in the theory. However, Γ_p dominates Γ_Q for a light nucleus such as ^{16}O and, while the curves shown in Fig. 6 have $\Gamma_Q = 500$ keV, there is little change if Γ_Q is disregarded and set equal to zero. As usual with a particle-hole model, the calculated cross sections are too high (Fig. 6d).

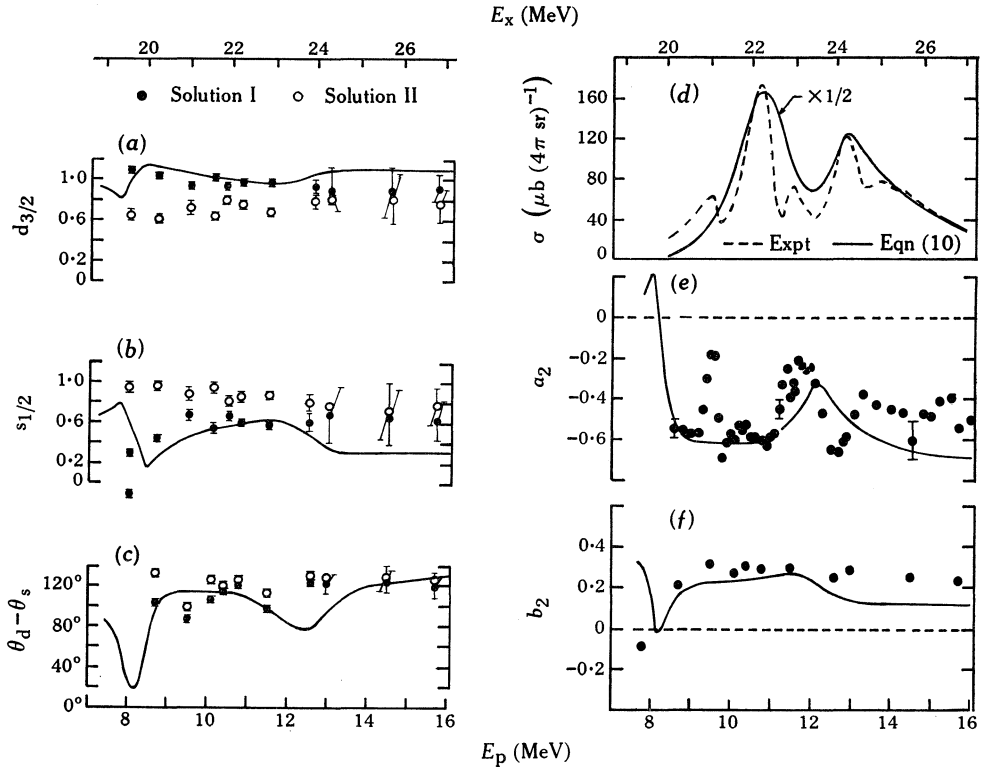


Fig. 6. Experimental data (points and dashed curve) and theoretical fits (solid curves) generated from equation (10) for the reaction $^{15}\text{N}(p, \gamma)^{16}\text{O}$.

(c) E1 Strength in ^{90}Zr

The splitting of the giant E1 strength into isospin components in medium mass nuclei was first observed and studied in ^{90}Zr in the reaction $^{89}\text{Y}(p, \gamma)^{90}\text{Zr}$ (Axel *et al.* 1967; Hanna 1969b; Hasinoff *et al.* 1969; Hughes and Fallieros 1969). It was shown that the $T_<$ strength is concentrated in the traditional broad giant resonance while the $T_>$ strength resides in sharp E1 analogue states superposed on the $T_<$ resonance (Hughes and Fallieros 1969). Just as the $T_<$ strength is pushed up to form the high-lying giant resonance, so the $T_>$ strength is transferred up from the lower analogue states (Shafroth and Legge 1968) to $T_>$ levels lying above the $T_<$ resonance (Fallieros

et al. 1965). These latter levels have been called the $T_>$ giant resonance. However, the $T_>$ strength is distributed over the 1^- analogue resonances, which coexist and interfere in a characteristic manner with the broad $T_<$ resonance (Ejiri and Bondorf 1968). It is my purpose now to discuss the two isospin components and their coexistence in terms of the polarized reaction $^{89}\text{Y}(p, \gamma)^{90}\text{Zr}$.

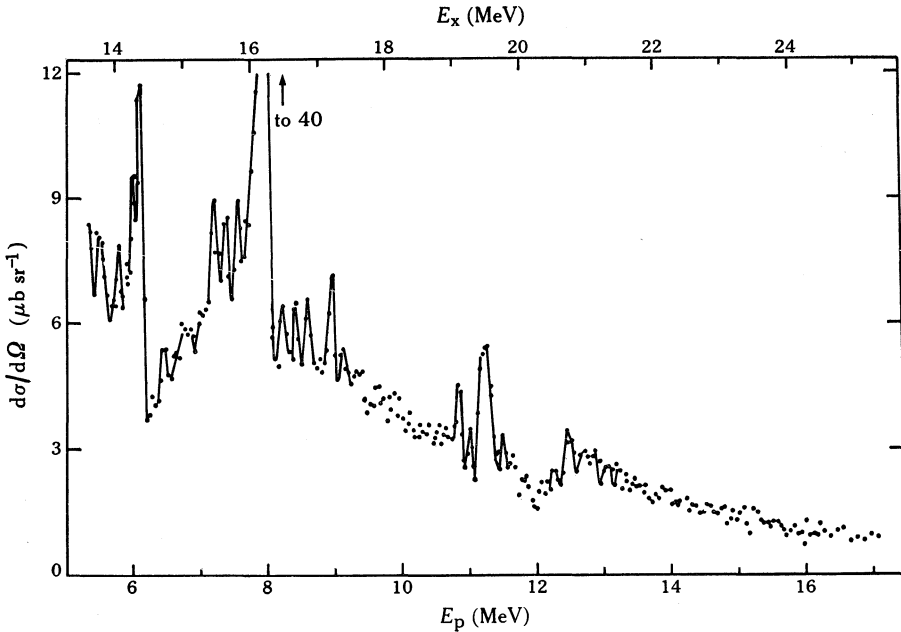


Fig. 7. The $\theta = 90^\circ$ yield from the unpolarized reaction $^{89}\text{Y}(p, \gamma_0)^{90}\text{Zr}$, showing the $T_<$ GDR and the $T_>$ analogue components.

Fig. 7 shows the 90° yield of the unpolarized reaction $^{89}\text{Y}(p, \gamma_0)^{90}\text{Zr}$ and nicely illustrates the above remarks. The broad $T_<$ resonance can be seen stretching from $E_x = 14.5$ to 25 MeV, with its peak at 16 MeV (the rise below 14.5 MeV can be attributed to the closing of the neutron channel and to interference with the analogue resonance at 14.43 MeV). Superposed on this resonance are sharp analogue states which comprise the $T_>$, $E1$ strength. These levels, located at $E_x = 14.43$, 16.28 , 19.45 and 20.7 MeV, produce considerable fine structure in their vicinity, either by enhancement of fine structure in the $T_<$ GDR or through some other mechanism. It is of course possible that other analogue states exist in this fine structure or are weakly present elsewhere. The other manner in which the analogues interact with the $T_<$ GDR is through interference (Hasinoff *et al.* 1973). We now ask: what can be learned about these isospin components and their coexistence from a 'complete experiment' (i.e. one including proton polarization)?

The analysing power of photons emitted from the giant resonance of ^{90}Zr was measured with the polarized proton capture reaction on ^{89}Y from $E_p = 6.15$ MeV to 12.92 MeV at $\theta_\gamma = 45^\circ, 90^\circ$, and 135° . The experimental technique was entirely similar to that used in the study of ^{16}O . The target was a self-supporting metal foil. Measurements were made on each of the analogue resonances and between the resonances. The results are shown in Fig. 8. The observed analysing power on the

resonance at $E_p = 6.15$ MeV is consistent with zero, indicating negligible interference in the proton channel. At higher energies, $\mathcal{A}(\theta)$ assumes a clear $P_{1/2}(\theta)$ dependence consistent with dipole radiation. The values of b_2 derived from these data are shown in Fig. 9 along with curves of A_0 , a_1 and a_2 from Hasinoff *et al.* (1973).

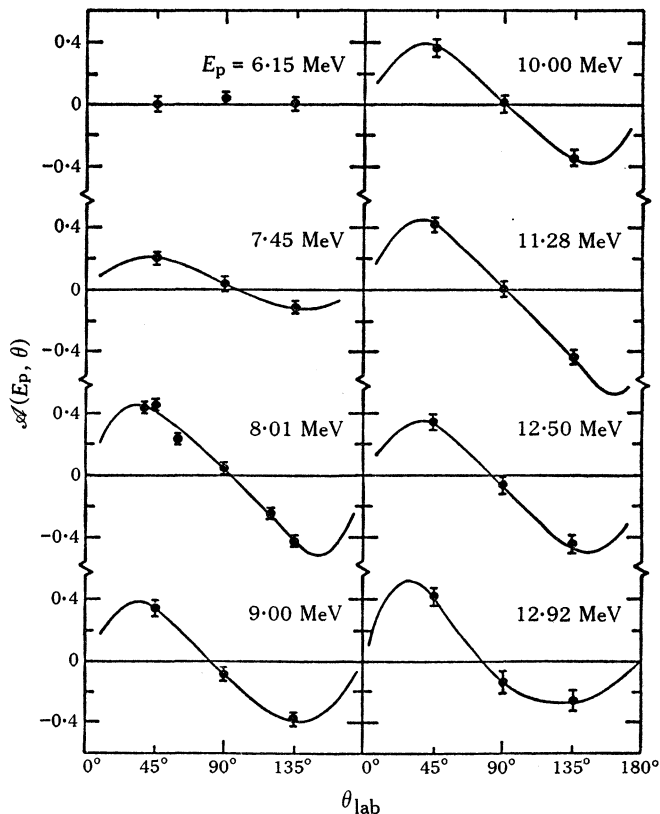


Fig. 8. Measured analysing powers $\mathcal{A}(\theta)$ for the polarized reaction $^{89}\text{Y}(p, \gamma_0)^{90}\text{Zr}$ plotted at eight selected energies E_p corresponding to both $T_<$ and $T_>$ components.

Since the J^π of ^{89}Y is $1/2^-$, the same as for ^{15}N , the equations (7), (8) and (9) given above for ^{16}O can be used for ^{90}Zr . The solutions I and II, obtained for $s_{1/2}$, $d_{3/2}$ and $\phi_d - \phi_s$ at each energy are also shown in Fig. 9. We observe the remarkable fact that not only the channel amplitudes but also their phase differences remain almost constant throughout the main part of the GDR including the $T_>$ resonances. However, an intriguing situation presents itself: if the lowest analogue resonance is predominantly s wave, as assigned in elastic proton scattering, and if we wish to have the preferred solution I (which is predominantly d wave) in the main part of the GDR, then solution I and solution II must cross between the s-wave analogue and the GDR. This point is under current investigation.

Solution I which gives about 90% d-wave and 10% s-wave capture in the (p, γ_0) channel is preferred since it agrees with the basic feature of the particle-hole model. However, this mixture remains approximately constant through the region including

the d-wave analogue resonance at $E_p = 8.01$ MeV and also the higher $T_>$ components of the giant resonance. The implication is that one mixture of configurations is responsible for the entire giant resonance, including the $T_>$ components. It may be possible to explain this pervasive feature of the E1 strength, as in the case of ^{16}O , by means of the doorway model.

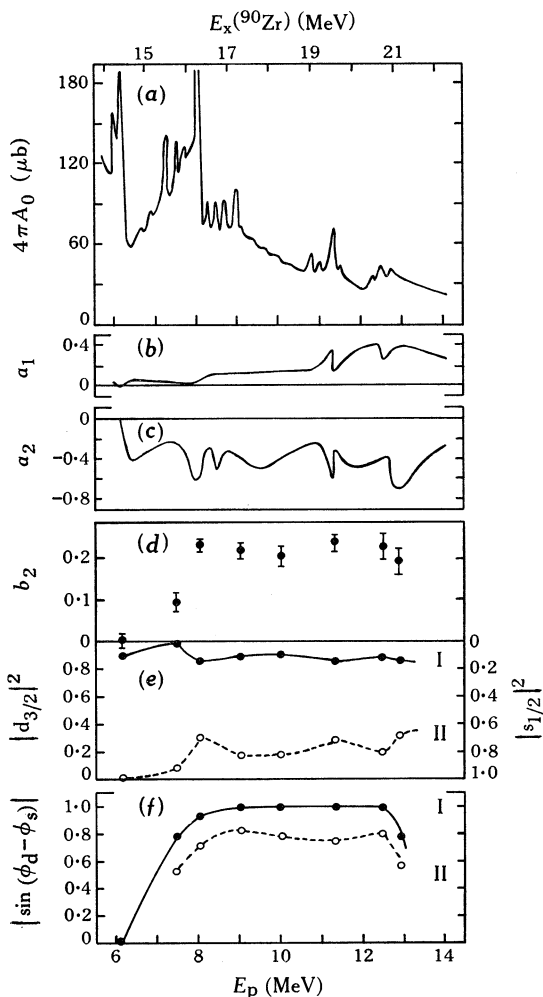


Fig. 9. Summary of E1 information on the GDR in $^{89}\text{Y}(p, \gamma)^{90}\text{Zr}$. The two solutions for the proton channel are indicated by I and II.

(d) E1 Resonance in ^4He

The theoretical and experimental work on the reaction $^3\text{H}(p, \gamma)^4\text{He}$ and its inverse have established several interesting features. The experimental E1 cross section exhibits a broad maximum (see Fig. 10a) even after allowance is made for kinematical and penetrability factors (Meyerhof *et al.* 1970). The angular distribution of the E1 radiation in the region of the broad maximum is almost pure $\sin^2 \theta$ corresponding to a strong contribution from the channel spin $S = 0$ state in the initial-particle channel,

and a small contribution from the $S = 1$ state. On the theoretical side, while it has been possible to analyse many of the features occurring in the particle channels such as ${}^3\text{H}(p, p){}^3\text{H}$ and ${}^3\text{H}(p, n){}^3\text{He}$ by means of a resonance theory involving excited levels in ${}^4\text{He}$ (Barit and Sergejev 1967; Werntz and Meyerhof 1968), this has been only partially successful when applied to the capture reaction ${}^3\text{H}(p, \gamma){}^4\text{He}$ (Crone and Werntz 1969; Meyerhof *et al.* 1970). In particular the distribution and the mixing of the singlet and triplet strength have not been unambiguously given.

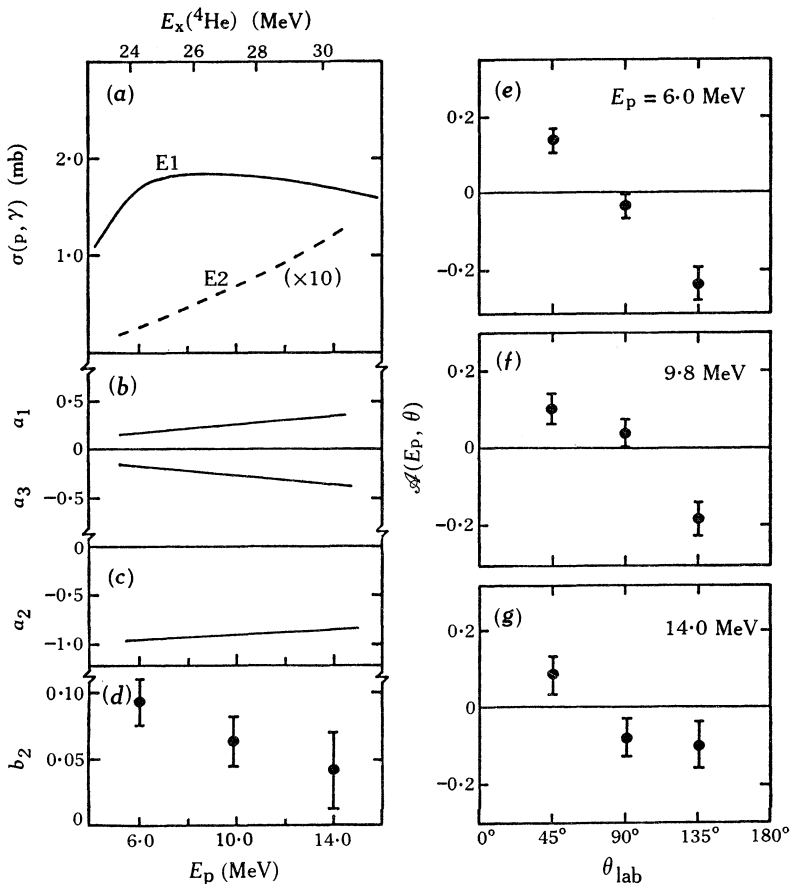


Fig. 10. Summary of information on the GDR in ${}^3\text{H}(p, \gamma){}^4\text{He}$. The dashed curve in (a) shows the E2 component ($\times 10$) of the yield, as estimated from the coefficients a_1 and a_3 alone.

To obtain a better understanding of the E1 cross section, the polarized proton capture reaction ${}^3\text{H}(p, \gamma){}^4\text{He}$ has been studied by observing the asymmetry produced in the angular distribution of the γ rays, as described above. By combining these new measurements with existing angular distribution data for the unpolarized reaction, solutions have been obtained for the $S = 0$ and $S = 1$ photoproton amplitudes and their relative phases.

The experimental technique was similar to that used in the experiments discussed above. The ${}^3\text{H}$ target consisted of 3 Ci of ${}^3\text{H}$ adsorbed in 3 mg cm^{-2} of erbium

mounted on a 2 mg cm^{-2} platinum backing. After passing through this target the beam was dumped behind shielding as before.

The analysing power $\mathcal{A}(E, \theta)$ was measured at laboratory angles of 45° , 90° and 135° , at proton bombarding energies $E_p = 6.0, 9.8$ and 14.0 MeV . The results are shown in Figs 10e–10g. Because of the smooth dependence of the cross section on energy, the measurements were made at only three widely spaced energies. The results show that, at the lower energies $E_p = 6.0$ and 9.8 MeV , $\mathcal{A}(\theta)$ has a pronounced $P_2^1(\theta)$ dependence which is consistent with predominant E1 radiation. At $E_p = 14.0 \text{ MeV}$ there is evidence of $P_1^1(\theta)$ and $P_3^1(\theta)$ terms corresponding to E1–E2 interference. Measurements of $\mathcal{A}(\theta)$ at just the three angles $45^\circ, 90^\circ$ and 135° are sufficient to determine the coefficient b_2 and to establish that b_1 and b_3 are not dominant over b_2 . At each energy the coefficient b_2 was determined from the measured value of $\mathcal{A}(\theta)$ and from $\sigma(\theta)/A_0$ obtained from the coefficients a_1, a_2 and a_3 given by Meyerhof *et al.* (1970). The values obtained for b_2 are shown in Fig. 10d. For completeness, a summary of a_1, a_2, a_3 and the total yield is included in Figs 10b, 10c and 10a.

We now pass from the coefficients a_2 and b_2 to the complex amplitudes of the proton channels in ${}^3\text{H}(p, \gamma){}^4\text{He}$, expressed in an *LS* coupling notation. Since only incident waves with $l = 1$ can form a 1^- state in ${}^4\text{He}$ we have only two amplitudes

$${}^3\text{P}_1 \exp(i\phi_1) \quad \text{and} \quad {}^1\text{P}_1 \exp(i\phi_0),$$

corresponding to the triplet ($S = 1$) and singlet ($S = 0$) channel spins. For E1 radiation we obtain

$$a_2 = 0.5({}^3\text{P}_1)^2 - ({}^1\text{P}_1)^2, \quad b_2 = -0.71 {}^3\text{P}_1 {}^1\text{P}_1 \sin(\phi_0 - \phi_1), \quad 1 = ({}^3\text{P}_1)^2 + ({}^1\text{P}_1)^2.$$

As was the case for ${}^{16}\text{O}$ and ${}^{90}\text{Zr}$, the coefficients a_2 and b_2 serve to fix the amplitudes and their relative phase in the proton channel.

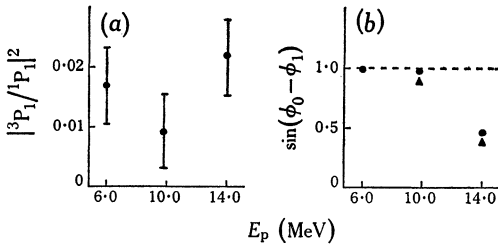


Fig. 11. Solutions obtained for the proton channel in ${}^3\text{H}(p, \gamma){}^4\text{He}$. The triangles are predictions derived from one set of phase shifts in ${}^3\text{H}(p, p){}^3\text{H}$.

As can be seen in Fig. 10a, the E2 contribution to the cross section is not negligible at the higher energies. Thus, in obtaining the dipole amplitudes, it is necessary to take this quadrupole contribution into account. This can be done in a straightforward way, and values for ${}^3\text{P}_1, {}^1\text{P}_1$ and $(\phi_0 - \phi_1)$ can be extracted from the data presented here. These are shown in Fig. 11: the triplet to singlet intensity ratio $|{}^3\text{P}_1/{}^1\text{P}_1|^2$ is plotted at three energies in Fig. 11a, and the quantity $\sin(\phi_0 - \phi_1)$ is shown (solid dots) in Fig. 11b. The errors indicated for the intensity ratios are rough estimates based on the general accuracy of the data.

From these results we obtain the following important conclusions concerning the proton configurations in the reaction ${}^3\text{H}(p, \gamma){}^4\text{He}$:

- (1) The triplet contribution is very small throughout the GDR ($E_x = 24 \rightarrow 30 \text{ MeV}$), i.e. less than 3%.

- (2) Within the present accuracy of the measurements the configuration does not change markedly throughout the GDR.
- (3) The phase difference between the singlet and triplet amplitudes is large.
- (4) As observed for ^{16}O , the major variation in the configuration is in the phase difference and not in the amplitudes.

The very small contribution of the triplet state is consistent with our simplest notions of the E1 strength in ^4He (and other nuclei) but is not well represented by the more elaborate theories.

The solid triangles shown for $\sin(\phi_0 - \phi_1)$ in Fig. 11b are the predictions obtained for the (p, γ) phase shifts from one set of the proton elastic scattering phase shifts of Hardekopf *et al.* (1972). The agreement is excellent. The prediction obtained from the second set of phase shifts fails to give agreement at the highest energy and this set of phase shifts can probably be eliminated. Thus, the polarized (p, γ) measurements can be used to fix the proton configuration not only in the (p, γ) reaction but possibly also in the (p, p) elastic scattering.

4. Giant M1 Resonances

Information on the giant M1 resonances is now rather extensive and exists all the way from mass 8 to 208. The methods which have been used to study the M1 resonance can be summarized as follows:

(1) Capture Reactions (X, γ) , where X stands for a nucleon or nucleus. Early work was not directed specifically at locating and studying the M1 strength. In recent years the work, principally at Stanford, Argonne and Orsay, has investigated the M1 strength of the $T_{>}$ and $T_{>>}$ levels of the light nuclei (Hanna 1969a). Some levels have also been studied by reactions of the type $(X, Y\gamma)$.

(2) Gamma-ray Fluorescence (γ, γ') . These investigations of M1 strength are represented by the early studies at NBS (Hayward and Fuller 1957) and Illinois (Kuehne *et al.* 1967) and more recent work at Bartol (Swann 1974).

(3) Inelastic Electron Scattering at 180° . The use of 180° scattering to sort out magnetic from electric multipoles was pioneered at Stanford (Barber 1962) and has recently been effectively continued at the Naval Research Laboratory (Fagg 1973) and at Darmstadt (Pitthan and Walcher 1971; Pithan 1973).

(4) Photoneutron Process (γ, n) . This process has been used at Livermore (Bowman *et al.* 1970), Argonne (Jackson 1973) and Harwell (Winhold *et al.* 1973) to give valuable information above the neutron threshold in heavy nuclei. Information comes also from the inverse (n, γ) reaction (Bollinger 1973).

A survey of the M1 strength observed in nuclei is contained in Figs 12, 13 and 14, and the pertinent references are given in Table 1.

(a) Light Nuclei

Let us first consider the odd-odd nuclei which appear to fall in a rather special category. It is unfortunate that not many of these nuclei have been studied, as they are of considerable interest because of the presence of the unpaired neutron and proton in their ground state. The three examples shown in Fig. 12 all come from the $1p$ shell and illustrate three types of behavior. In ^6Li , 90% of the M1 strength is

Table 1. Sources of data on M1 strengths

| Nucleus | References* | Nucleus | References* | Nucleus | References* |
|--------------------|-------------|---------------------|-------------|---------------------|--------------|
| ${}^6\text{Li}$ | 1, 2, 3, 4 | ${}^{25}\text{Mg}$ | 4, 7 | ${}^{113}\text{Cd}$ | 9 |
| ${}^8\text{Be}$ | 1, 2, 3 | ${}^{25}\text{Al}$ | 1, 7 | ${}^{114}\text{Cd}$ | 12 |
| ${}^9\text{Be}$ | 1, 3, 4 | ${}^{26}\text{Mg}$ | 4, 7 | ${}^{116}\text{In}$ | 13 |
| ${}^9\text{B}$ | 1, 3 | ${}^{28}\text{Si}$ | 4, 6, 7 | ${}^{117}\text{Sn}$ | 8, 9 |
| ${}^{10}\text{B}$ | 2, 3, 4 | ${}^{32}\text{S}$ | 4, 6, 7 | ${}^{118}\text{Sn}$ | 13 |
| ${}^{11}\text{B}$ | 1, 3, 4 | ${}^{36}\text{Ar}$ | 4, 7 | ${}^{119}\text{Sn}$ | 8, 9 |
| ${}^{12}\text{C}$ | 1, 2, 3, 4 | ${}^{40}\text{Ca}$ | 4, 7 | ${}^{120}\text{Sn}$ | 13 |
| ${}^{13}\text{C}$ | 1, 3, 4 | ${}^{44}\text{Ti}$ | 7 | ${}^{122}\text{Sb}$ | 13 |
| ${}^{13}\text{N}$ | 1, 3 | ${}^{56}\text{Fe}$ | 8 | ${}^{136}\text{Ba}$ | 14 |
| ${}^{14}\text{C}$ | 4 | ${}^{57}\text{Fe}$ | 8 | ${}^{139}\text{La}$ | 15 |
| ${}^{14}\text{N}$ | 2, 3, 4 | ${}^{58}\text{Ni}$ | 4 | Ce | 15 |
| ${}^{15}\text{N}$ | 1, 3, 4 | ${}^{87}\text{Sr}$ | 9 | ${}^{141}\text{Pr}$ | 15 |
| ${}^{17}\text{F}$ | 5 | ${}^{88}\text{Sr}$ | 10, 11 | ${}^{197}\text{Au}$ | 4, 16 |
| ${}^{20}\text{Ne}$ | 1, 4, 6 | ${}^{90}\text{Zr}$ | 4 | ${}^{206}\text{Pb}$ | 4 |
| ${}^{21}\text{Na}$ | 7 | ${}^{91}\text{Zr}$ | 9 | ${}^{207}\text{Pb}$ | 8 |
| ${}^{22}\text{Ne}$ | 4 | ${}^{97}\text{Mo}$ | 9 | ${}^{208}\text{Pb}$ | 4, 8, 17, 18 |
| ${}^{24}\text{Mg}$ | 1, 4, 6, 7 | ${}^{106}\text{Pd}$ | 12 | | |

* References and Notes:

- 1, Hanna (1969a).
- 2, Kurath (1963).
- 3, Ajzenberg-Selove and Lauritsen (1974) for $A = 5-10$;
Ajzenberg-Selove (1975) for $A = 11$ and 12;
Ajzenberg-Selove (1970) for $A = 13-15$;
Ajzenberg-Selove (1971) for $A = 16$ and 17;
Ajzenberg-Selove (1972) for $A = 18-20$.
- 4, Fagg (1975).
- 5, Harakeh *et al.* (1975).
- 6, Hanna (1974).
- 7, Endt and Van der Leun (1973).
- 8, Jackson (1973).
- 9, Winhold *et al.* (1973).
- 10, Metzger (1971).
- 11, Cecil *et al.* (1973).
- 12, Smither and Bollinger (1969);
Bollinger and Thomas (1970).
- 13, Bartholomew *et al.* (1973).
- 14, Bollinger (1973).
- 15, Pitthan and Walcher (1971);
Pitthan (1973).
- 16, Buskirk *et al.* (1973).
- 17, Bowman *et al.* (1970).
- 18, Swann (1974).

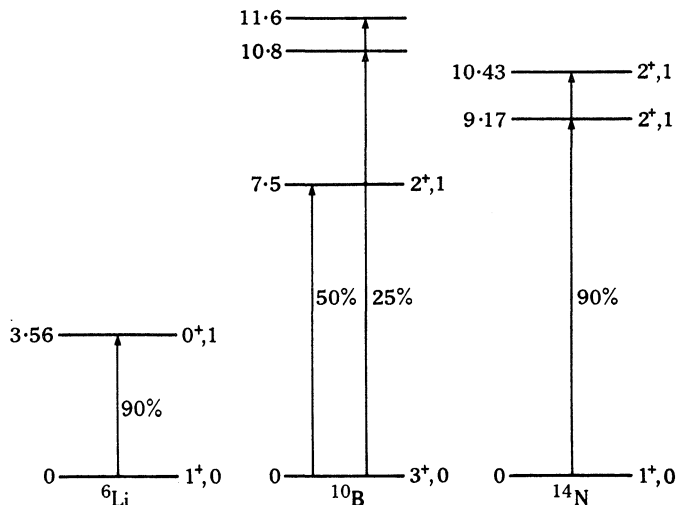


Fig. 12. Giant M1 strength in odd-odd nuclei (% sum rule). References may be found in Table 1.

concentrated in a single low-lying level (Cohen and Tobin 1959): the spin- and isospin-flip transition of the 'deuteron' type. In ^{10}B , in the middle of the shell, the strength is spread over levels rather widely spaced (Edge and Peterson 1962; Spamer 1966; L. W. Fagg, personal communication) but there is still a tendency toward concentration into a single level. In ^{14}N , the shell model predicts the M1 strength to be concentrated in a single level, which in nature becomes mixed with a neighbouring level (Warburton and Pinkston 1960; Rose 1962).

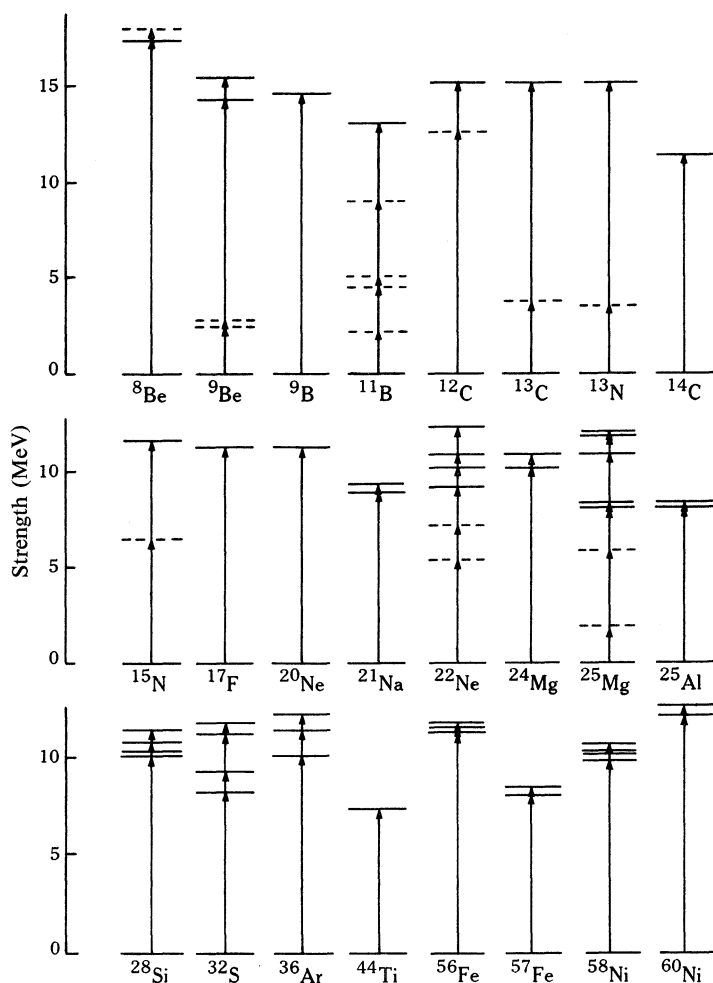


Fig. 13. Giant M1 strength in nuclei from $A = 8$ to 60. References may be found in Table 1.

The strengths of the transitions, given in terms of the M1 sum rule, have been derived from various measurements with γ -ray, electron-scattering and capture reactions. The sum rule strength for each nucleus is taken simply as the total M1 strength predicted by the shell model calculation of Kurath (1963).

Fig. 13 surveys the M1 strength observed in other nuclei from $A = 8$ to 60. Where known, the isospin of the level is indicated by a solid line (T_+) or a dashed line (T_-).

I cite here only some typical examples and interesting features of these transitions. The M1 transition in ^8Be , observed by the (p, γ) reaction (Hafstad *et al.* 1936), was the first giant resonance of any kind observed. The resonance in ^{12}C was found in particle reactions many years ago (Cohen *et al.* 1954) and has since been studied by many reactions, and is often used as a standard. The transitions in the odd-mass nuclei have been studied principally by proton capture reactions but also by γ -ray decay following nuclear reactions and by electron scattering. The M1 levels in the $4N$ nuclei have been investigated by γ -ray fluorescence, by electron scattering and by γ -ray decay from the $T = 2$ levels above.

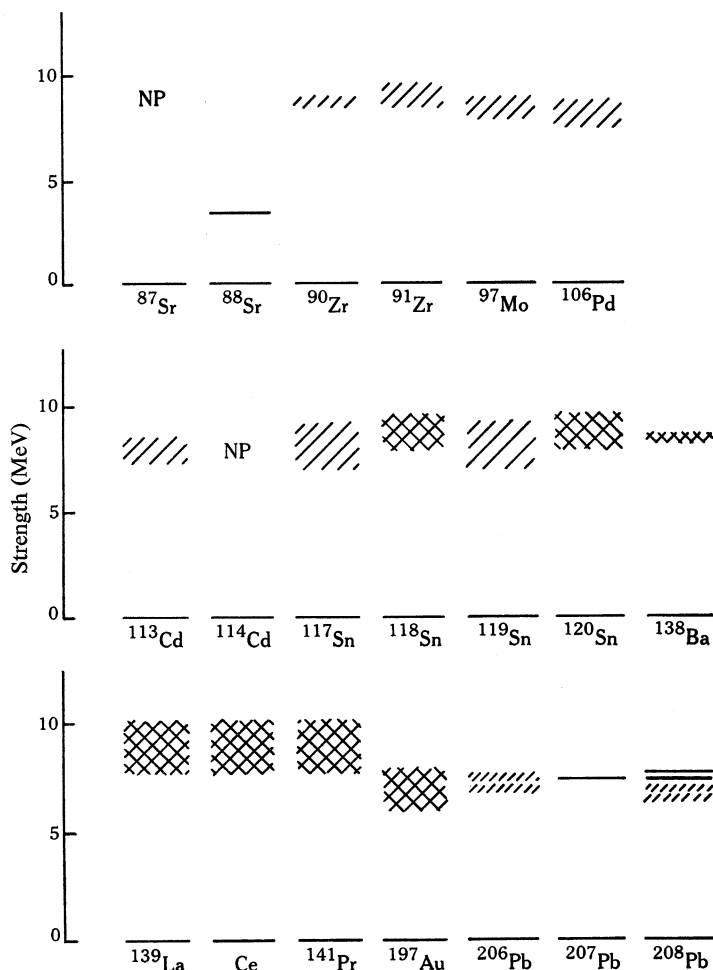


Fig. 14. M1 excitation in nuclei from $A = 87$ to 208. The absence of any particular peaking is indicated by NP. References may be found in Table 1.

A typical example of the excitation of an M1 giant resonance by electron scattering is shown beautifully (Fagg 1973) by the excitation of a single level in ^{20}Ne (Fig. 15). The strength of this excitation is discussed below. The partial level diagram for $A = 24$ shown in Fig. 16 illustrates the method of studying the M1 levels by observing

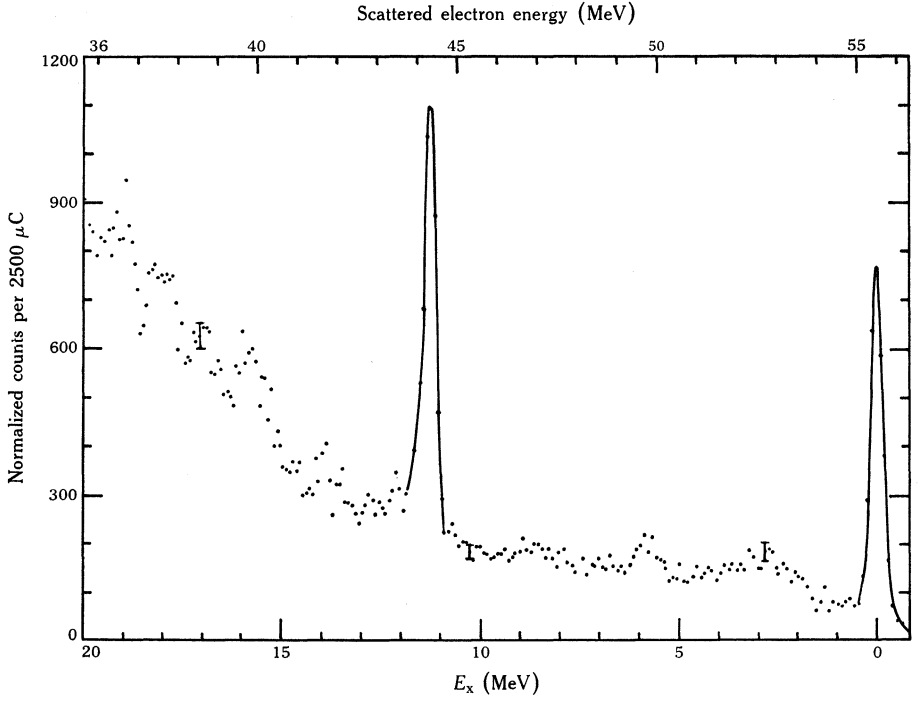


Fig. 15. M1 excitation in ^{20}Ne observed in electron scattering at 180° . The data are for $E_0 = 56.0$ MeV (Fagg 1973).

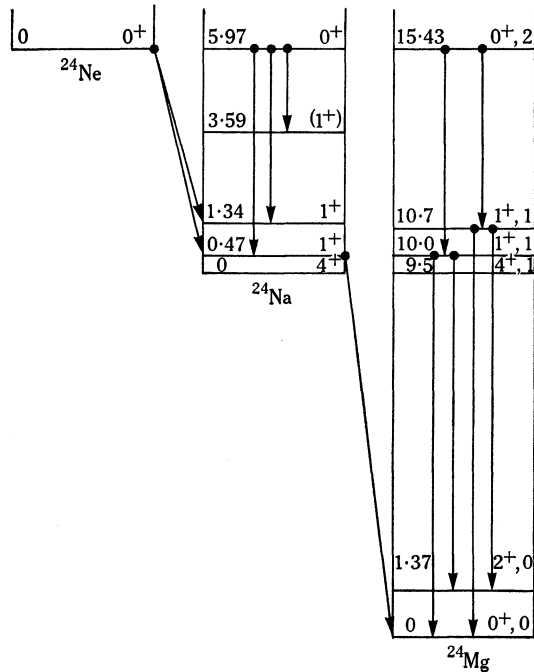


Fig. 16. M1 γ -ray and β -particle transitions in $A = 24$ nuclei (Hanna 1974).

the radiative decay of the 0^+ , $T = 2$ level formed in proton capture (Riess *et al.* 1967). It is of course just as good to study these levels by excitation from above as from below. The level diagram also shows the importance of studying the γ -ray and β -particle analogues of the M1 decays. By comparing the γ -ray analogues one can test basic selection rules (Hanna 1969a). On the other hand, the β -particle analogues measure the spin part of the transition and allow one to assess the importance of the orbital contribution to the M1 transition.

We note the lack of any reported M1 strength in the 'closed-shell' nuclei ^{16}O and ^{40}Ca , where the in-shell spin-flip transitions are inhibited. The location of M1 strength in these nuclei is an important experimental problem.

The strengths of many of the M1 transitions shown in Fig. 13 have been compared with the Kurath (1963) sum rule

$$61 \sum \Gamma_i/E_i^2 = -a \langle 0 | \sum l_j \cdot s_j | 0 \rangle, \quad T = 0 \rightarrow T = 1, \quad (11)$$

where Γ_i and E_i are the width and energy of the i th level, a is the spin-orbit coupling parameter, and $\langle || \rangle$ denotes the expectation value of the spin-orbit coupling in the ground state. One may insert the experimental values on the left-hand side of equation (11) and compare the sum with the right-hand side which represents the total expected M1 strength. A summary of such a comparison (Maruyama *et al.* 1974) based on electron scattering results is given in Table 2. In the sd shell $a \approx -2.0$ MeV. Two evaluations of the right-hand side of the sum rule (11) are given, where possible: case A, a value calculated from a complete j - j shell model picture, and case B, a value predicted from occupation numbers in the ground state obtained either from a large shell model calculation or from empirical evidence.

Table 2. Comparison of measured M1 strength with M1 sum rule

| Nucleus | $61 \sum \Gamma_i/E_i^2$ Experimental | $2 \langle 0 \sum l_j \cdot s_j 0 \rangle$ | |
|------------------|--|--|---------|
| | | Case A* | Case B* |
| ^{20}Ne | 5.5 | 8.0 | 3.14 |
| ^{22}Ne | 4.7 | 12.0 | 8.24 |
| ^{24}Mg | 14.1 | 16.0 | |
| ^{26}Mg | 19.6 | 20.0 | |
| ^{28}Si | 18.8 | 24.0 | 11.4 |

* Notes:

Case A. Calculated in the independent single-particle model.

Case B. For ^{20}Ne and ^{22}Ne , the occupation numbers are calculated from the sd shell model (B. H. Wildenthal, personal communication). For ^{28}Si , empirical values are used (Gove *et al.* 1968).

We see that for ^{24}Mg and ^{26}Mg the observed strength is close to exhausting the extreme j - j value. For ^{20}Ne and ^{22}Ne , the shell model calculations (B. H. Wildenthal, personal communication) indicate a strong reduction of the strength, which is in better agreement with experiment. For ^{28}Si , the measured strength lies between the limiting value and that obtained from occupation numbers in the ground state as derived from transfer reactions (Gove *et al.* 1968). We note, however, that this value is very sensitive to these occupation members. Discussions of the application of this

sum rule in the deformed model can be found in the original papers (Kurath 1963; Kuehne *et al.* 1967) or in reviews (e.g. Hanna 1969a).

Another important evaluation of the strengths of these M1 transitions can be made by comparing them to their analogue GT β transitions. D. Kurath (see Hanna 1969a) has reduced this comparison to the following expression

$$A(M1) = A(1 + 0.11 \langle |I| \rangle / \langle |s| \rangle)^2 A(GT), \quad (12)$$

where $A(M1)$ and $A(GT)$ are reduced matrix elements for the analogue M1 and GT transitions, $\langle |I| \rangle$ and $\langle |s| \rangle$ are the appropriate matrix elements of the orbital angular momentum operator and spin operator, and A is a constant determined only by the isospin of the levels involved.

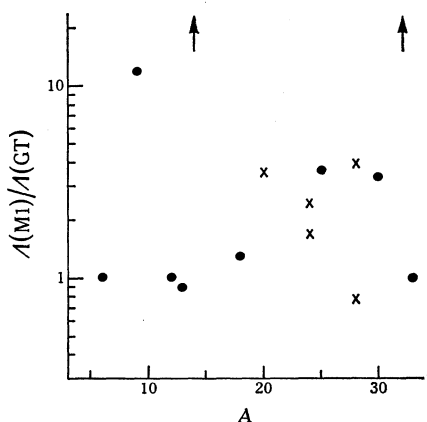


Fig. 17. Comparison of analogue γ -ray and β -particle transitions (Hanna 1974).

Fig. 17 shows the comparison for the M1 levels in the p and sd shells. The circles show $T = 0$ to $T = 1$ transitions and the crosses show $T = 1$ to $T = 2$ transitions. The units are such that $A(M1)/A(GT) = 1$ if $\langle |I| \rangle = 0$. We see that for several of the transitions the orbital contribution is small, but that in many cases it plays an important role in the M1 strength.

Throughout the sd shell there now exist many large shell model calculations. It is thus possible to compare many of the M1 transitions with the predictions of these calculations. Such a comparison (Hanna 1974) reveals generally good agreement, but many of the experimental data are not yet precise enough for a definitive comparison.

(b) Heavy Nuclei

A summary of M1 strength in the heavier nuclei is shown in Fig. 14. From $A = 87$ to 138, the work has been done principally with the (γ, n) reaction and many of the results are conflicting. In Fig. 14, uncertainty or a lack of confirmation is indicated by single hatching, while better established cases are shown by cross hatching. The designation NP signifies that no particular peaking is seen in the M1 strength. From $A = 139$ to 197, the results are taken from electron scattering measurements. A typical example (Pitthan and Walcher 1971; Pitthan 1973) is shown in Fig. 18, where the M1 resonance in Ce is the only one seen at 165° .

In the Pb region, the results come principally from (γ, n) and electron scattering measurements. Considerable strength was reported (Bowman *et al.* 1970) in the 7.8 MeV region by means of photoneutron measurements just above threshold. However, a recent measurement (Holt and Jackson 1975), in which the neutron polarization was determined, has reduced the number of levels in this region to only two, at 7.6 and 8.0 MeV. Strength at 7.5 MeV has also been identified in ^{207}Pb (Jackson 1973).

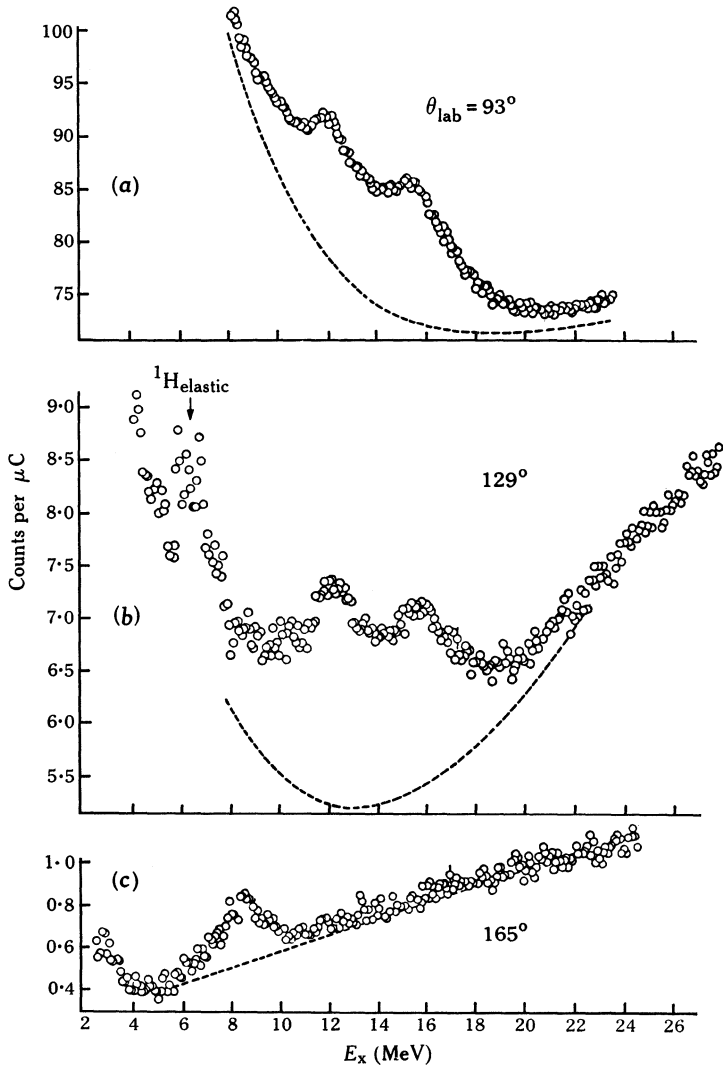


Fig. 18. Excitation of giant resonances in Ce by inelastic electron scattering. The data are for $E_0 = 65$ MeV (Pitthan and Walcher 1971; Pitthan 1973).

A resonance corresponding to this strength may also be present in electron scattering in ^{208}Pb and ^{206}Pb (Fagg *et al.* 1973; Lone 1974). However, more recent measurements on ^{208}Pb have identified most of this strength as M2 (Fagg *et al.* 1973; Lone 1974). The electron scattering also reveals possible M1 strength below the neutron threshold, as indicated by hatching at 7 MeV in ^{206}Pb and ^{208}Pb in Fig. 14.

In the past year [1974], the most interesting feature in ^{208}Pb was the report of a strong M1 level (5 eV) at 4.8 MeV observed in resonance fluorescence (Swann 1974). The assignment of this level was obtained by angular correlation and polarization measurements. However, it is very puzzling that this level has not been seen in electron scattering, and recently it was observed (G. T. Garvey, personal communication) in (α, α') , which indicates the level has natural parity, i.e. $J^\pi = 1^-$. Until this experimental disagreement is resolved the question of M1 strength in this region must be considered very doubtful.

The presence of such a strong level at 4.8 MeV would represent a very large and significant spreading of the M1 strength in ^{208}Pb , which would be due presumably to the interaction of the $h_{11/2} \rightarrow h_{9/2}$ proton transition with the $i_{13/2} \rightarrow i_{11/2}$ neutron transition (Vergados 1971). On the other hand, if these transitions are identified with the recently established levels at 7.6 and 8.0 MeV, then the spreading is very small and theory (J. Speth, personal communication) can account nicely for the observed strengths.

(c) Summary of Giant M1 Properties

In many of the cases shown in Figs 13 and 14, the levels have been observed by several methods; in others, different levels have been observed by different methods. It should also be emphasized that in many nuclei all the M1 strength has not been located. In general, no attempt has been made to assess critically the evidence, nor to evaluate the total reported M1 strength. Instead, these figures have been presented to display the flavour and the extent of the M1 strength already observed in those nuclei included.

It is instructive to associate the strong transitions in Figs 13 and 14 with the strong spin-flip transitions provided by the shell model. We note from the sum rule discussed above that the major strength should reside in the spin-flip transitions of maximum l . These transitions, together with the associated ranges in the numbers A_p and A_n of protons and neutrons respectively, are:

| | $p_{3/2} \rightarrow p_{1/2}$ | $d_{5/2} \rightarrow d_{3/2}$ | $f_{7/2} \rightarrow f_{5/2}$ | $g_{9/2} \rightarrow g_{7/2}$ | $h_{11/2} \rightarrow h_{9/2}$ | $i_{13/2} \rightarrow i_{11/2}$ |
|-------|-------------------------------|-------------------------------|-------------------------------|-------------------------------|--------------------------------|---------------------------------|
| A_p | 5...15 | 17...41 | 41...85 | 93...139 | 197...211 | |
| A_n | 5...15 | 17...39 | 39...67 | 73...111 | 117...149 | 195...211 |

From the evidence presented in Figs 13 and 14 we may extract the basic properties of the giant M1 resonances. These may be summarized, along with the E1 properties for comparison, as follows (subject to exceptions to the E1 properties and discussion of the M1 properties given in the text):

| Resonance | E_x | Strength | Γ/E_x |
|-----------|--------------------------------|------------------|--------------|
| E1 | $77 A^{-1/3}$ | $60 NZ A^{-1/3}$ | 0.2 |
| M1 | $(30 \rightarrow 45) A^{-1/3}$ | \sim sum rule | ~ 0.2 |

The location of M1 strength may not be as systematic as that of the E1 strength. This may be due in part to incomplete evidence, but may also arise from a real variation depending on the nuclear type or species ($4N, 4N \pm 1$, etc.); the 'anomalous' behaviour of the odd-odd nuclei was noted above. There is also some tendency for the M1 strength to be located at $45 A^{-1/3}$ in the heavy nuclei and at a lower value of $(30 \rightarrow 35) A^{-1/3}$ in the light nuclei. Until the evidence is more definitive we portray the

M1 strength in a band at $(30 \rightarrow 45)A^{-1/3}$ in Fig. 1 and in the summary tabulation. This does not mean, however, that the M1 strength is spread over the whole range in any given nucleus.

Wherever the total M1 strength is known and the relevant properties of the ground state are also known, either theoretically or experimentally, the strength is found to practically exhaust the sum rule. This remark applies to a number of cases in the light nuclei. Much more systematic work needs to be done in the heavy nuclei. But the data accumulated so far suggest that a similar concentration of strength may be localized in the giant M1 resonance of the heavy nuclei.

The spreading of the M1 strength appears to be similar to that of the E1 strength, although the data are still not complete enough for a quantitative comparison. In the light nuclei, the level density is low enough that the strength is usually concentrated in one or a few levels, but the spreading may turn out to be about the same as in the heavy nuclei. The spreading of the M1 strength, which in zero approximation is concentrated in pure shell-model configurations, is of considerable importance as it gives information on the spin dependence of the nuclear force.

Isospin splitting of the M1 strength can be seen in Fig. 13. In the self-conjugate nuclei, $4N$ and $4N+2$, the well-known selection rule puts most of the strength in the $T = 1$ transitions. Isospin mixing can be seen in the two close levels in ${}^8\text{Be}$ and ${}^{12}\text{C}$. In the other nuclei, the splitting between $\Delta T = 1$ and $\Delta T = 0$ strength is often quite large, but a systematic study has not yet been carried out.

5. Giant E2 Strength

The recent interest in the study of the E2 strength has stemmed from the observation of compact isoscalar E2 resonances below the well-known E1 resonance in electron scattering by Pitthan and Walcher (1971) and their identification in inelastic proton scattering (Lewis and Bertrand 1972; Bertrand *et al.* 1973). It appeared at first that these resonances were of a different nature from the E2 strength seen earlier in proton capture experiments in the lighter nuclei. However, extensive work during the past year [1974] on capture reactions (see Progress Report, Nuclear Physics Laboratory, Stanford University 1974; Kuhlmann *et al.* 1975) and inelastic alpha scattering (see Progress Report, Cyclotron Institute, Texas A&M University 1974; Moss *et al.* 1975) has greatly clarified the picture. In the light nuclei, it seems now well established that much of the E2 strength falls in or above the E1 resonance, but that in fact the E2 strength is spread out over a wide region. In the heavier nuclei, the compact isoscalar E2 resonance is well established but many measurements give its strength as much smaller than the E2 sum rule (values of 10% \rightarrow 100% are reported). Until these measurements are clarified, there exists the possibility that the E2 strength may also be spread out in the heavy nuclei.

The existence of an isoscalar E2 resonance was predicted on quite general grounds by Bohr and Mottelson (1975; see also Suzuki 1973) at a position of about $60 A^{-1/3}$ MeV. Recently, extensive shell-model calculations (Krewald *et al.* 1974; S. Krewald, personal communication; Bertsch and Tsai 1975) based on 1p-1h excitations (see Fig. 19) have been carried out for spherical nuclei such as ${}^{16}\text{O}$, ${}^{40}\text{Ca}$, ${}^{90}\text{Zr}$ and ${}^{208}\text{Pb}$. These calculations also place the strength at about $60 A^{-1/3}$ MeV. It is implicit in all these calculations that this resonance, together with the well-known first excited 2^+ state, will exhaust the isoscalar E2 sum rule.

In this paper we use the Gell-Mann–Telegdi sum rule for the isoscalar E2 strength:

$$\int (\sigma/E^2) dE = 0.255(Z^2/A)\langle R^2 \rangle \quad \mu\text{b MeV}^{-1}$$

$$= 0.22 Z^2/Z^{1/3} \quad \mu\text{b MeV}^{-1}, \quad (13)$$

where we have taken

$$\langle R^2 \rangle = 0.6(1.2 A^{1/3})^2 \quad \text{fm}^2.$$

We may classify the methods which have been used to study E2 strength as follows:

(1) Capture Reactions (X, γ). The first evidence for E2 strength came from angular distributions of (p, γ) reactions (Allas *et al.* 1964a). The (p, γ) work has continued (O'Connell *et al.* 1973) and been made much more definitive by the use of polarized protons at Stanford (Hanna *et al.* 1974). Important information has also been obtained from the (γ, p) process (Frederick *et al.* 1969). A great deal of evidence has been accumulated from the (α, γ) reaction at Argonne (Meyer-Schützmeister *et al.* 1968), Canberra (Watson *et al.* 1973; Foote 1974), Seattle (Snover *et al.* 1974a) and Stanford (see 1974 Stanford Progress Report cited above; Kuhlmann *et al.* 1975).

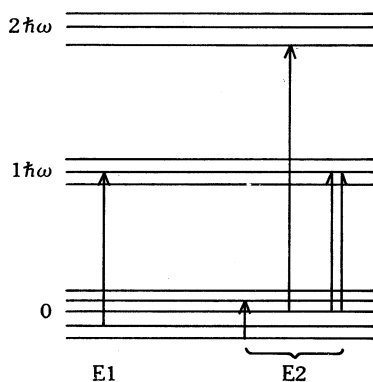


Fig. 19. Schematic E1 and E2 excitations in nuclei.

(2) Inelastic Electron Scattering (e, e'). The first isoscalar E2 resonances in heavy nuclei were observed at Darmstadt (Pitthan and Walcher 1971; Pitthan 1973). The work has since continued, chiefly at Darmstadt and at Sendai (Torizuka *et al.* 1973).

(3) Inelastic Scattering by Nuclear Particles (X, X'). The pioneering work with these reactions was carried out at Oak Ridge (Lewis and Bertrand 1972; Bertrand *et al.* 1973), where the isoscalar resonances were identified in earlier results from (p, p') scattering appearing in the literature as well as in current measurements. Subsequent work was carried out with (p, p') at Oak Ridge, Orsay (Marty *et al.* 1975) and Grenoble (Perrin *et al.* 1974), with ($^3\text{He}, ^3\text{He}'$) at Michigan State (Moalem *et al.* 1973), with (d, d') at Maryland (Chang *et al.* 1975), and with (α, α') at Texas A&M (see 1974 Texas A&M Progress Report cited above; Moss *et al.* 1975).

(a) (α, γ_0) Reaction

One of the most interesting features of the E2 strength observed in the light nuclei is the relatively great strength of the α_0 decay (where the barrier does not prohibit it) as observed by the inverse (α, γ) capture reaction. Measured in terms of their respective

sum rules, the α_0 decay from the E2 excitations is about 10 times more probable than from the E1 resonances. As we see below, however, the E2 strength that decays by α particles is spread out over low excitation energies and may indicate a 'different kind' of E2 strength.

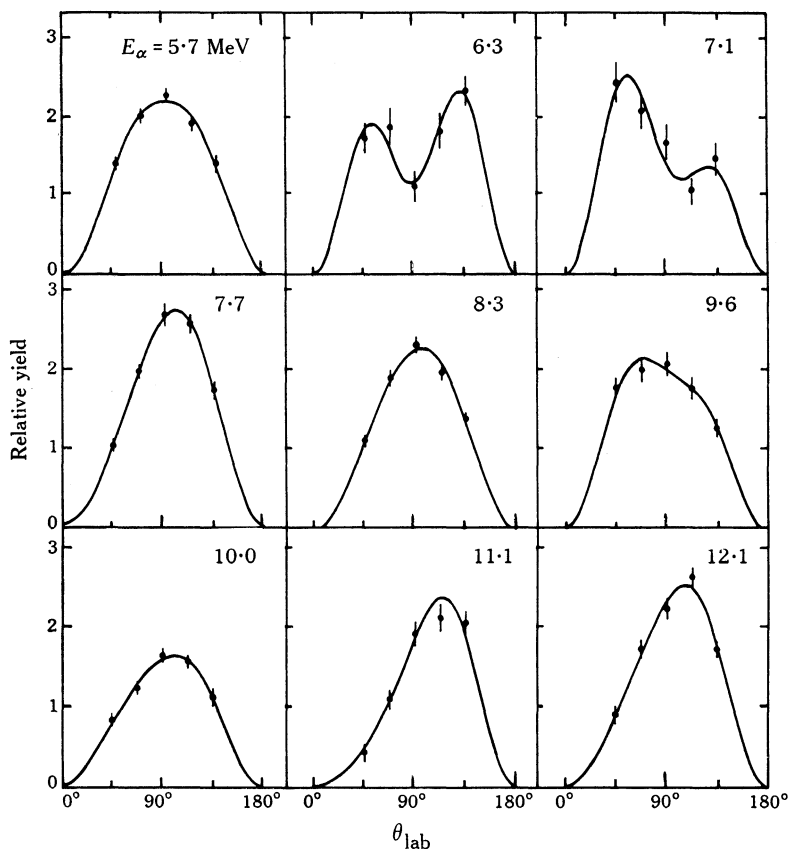


Fig. 20. Angular distributions from $^{28}\text{Si}(\alpha, \gamma)^{32}\text{S}$ (Kuhlmann *et al.* 1975).

In the (α, γ) , or (γ, α) , process on 0-spin nuclei, the E2 strength can be unambiguously separated from the E1 strength by means of angular distributions. A typical set of angular distributions (see 1974 Stanford Progress Report already cited; Kuhlmann *et al.* 1975) from the reaction $^{28}\text{Si}(\alpha, \gamma)^{32}\text{S}$ is shown in Fig. 20. The distributions range from almost pure dipole to those with substantial admixtures of quadrupole radiation. The E2-E1 interference causes the distributions to be asymmetric about 90° .

From (α, γ) measurements of this kind, the strength has been extracted from 0-spin nuclei from $A = 16$ to 60. References are given in Table 3 and the results are summarized in Figs 21 and 22. I emphasize that the E2 strength observed in these experiments is only that seen in the α_0 decay channel. Fig. 21 includes not only this ' α_0 strength' but also the total E2 strength measured in the bound and low-lying discrete resonances (as extracted from various compilations; Endt and Van der Leun 1973). The arrows mark the location at $63 A^{-1/3}$ of the compact isoscalar resonance

Table 3. Sources of data on E2 strengths from (α, γ) reactions

| Nucleus | References* | Nucleus | References* | Nucleus | References* |
|------------------|-------------|------------------|-------------|------------------|-------------|
| ^{16}O | 1 | ^{32}S | 2, 3, 4 | ^{44}Ti | 5 |
| ^{24}Mg | 2 | ^{34}S | 2 | ^{52}Cr | 4 |
| ^{26}Mg | 2 | ^{40}Ca | 4 | ^{60}Ni | 4 |
| ^{28}Si | 3,4 | ^{42}Ca | 4 | | |
| ^{30}Si | 3 | ^{44}Ca | 4 | | |

* References:

1, Snover *et al.* (1974a).

2, Prog. Rep. Nucl. Phys. Lab. Stanford Univ. 1974;

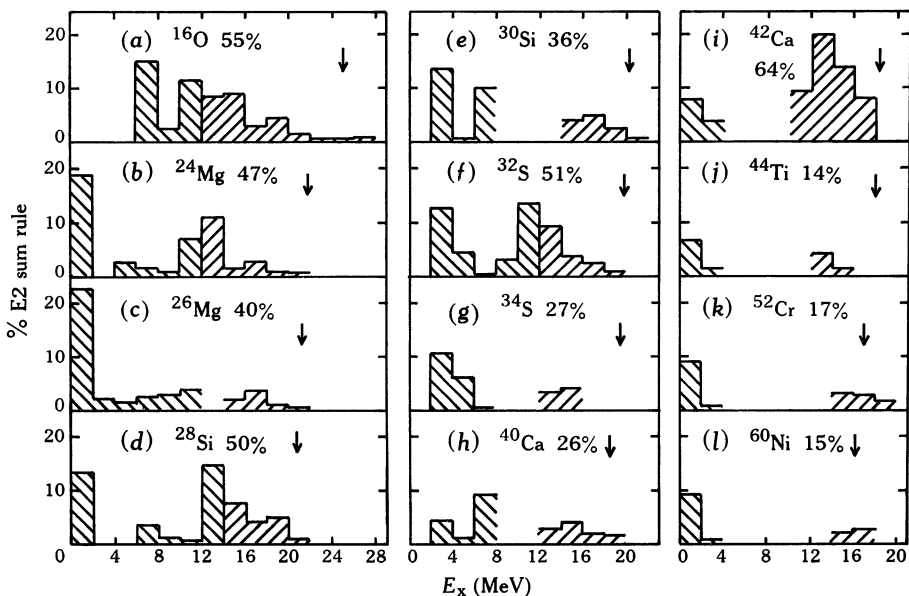
Kuhlmann *et al.* (1975).3, Meyer-Schützmeister *et al.* (1968).4, Watson *et al.* (1973); Foote (1974).5, Peschel *et al.* (1974).

Fig. 21. Summary of E2 strength observed in low-lying resonances and in (α, γ) reactions. The arrows locate $63 A^{-1/3}$ MeV. References may be found in Table 3.

observed in medium and heavy nuclei. We see that there is no indication of such a resonance in these data. The present evidence (see below) suggests that below ^{40}Ca such a compact resonance does not exist, while above ^{40}Ca the (γ, α_0) process does not reveal it, perhaps because of competition from other decay channels (Watson *et al.* 1973; Foote 1974) and suppression by the Coulomb barrier. In any case, the strength displayed in Fig. 21 is very large, averaging about 50% of the isoscalar E2 sum rule (wherever the data are reasonably complete), and is spread out over the region from the first 2^+ level up to $63 A^{-1/3}$. If one adds to the ' α_0 strength' any reasonable estimate of the E2 strength decaying into other channels, one concludes that a major portion of the isoscalar E2 sum rule is exhausted well below $63 A^{-1/3}$.

Fig. 22 summarizes the E2-E1 phase differences obtained from all the (α, γ) measurements. We note that in ^{16}O , below 20 MeV, the phase varies rapidly in

accordance with the resonant structures observed there. However, above 20 MeV, where a compact isoscalar resonance might exist, the phase is flat and featureless. This is true of all the other cases shown in Fig. 22. The arrows show possible locations for a compact E2 resonance, at either $63 A^{-1/3}$ MeV or at 3 MeV below the E1 resonance. This constant behavior of the E2–E1 phase difference is strong evidence that the E2 strength associated with α_0 decay does not participate in any compact resonance.

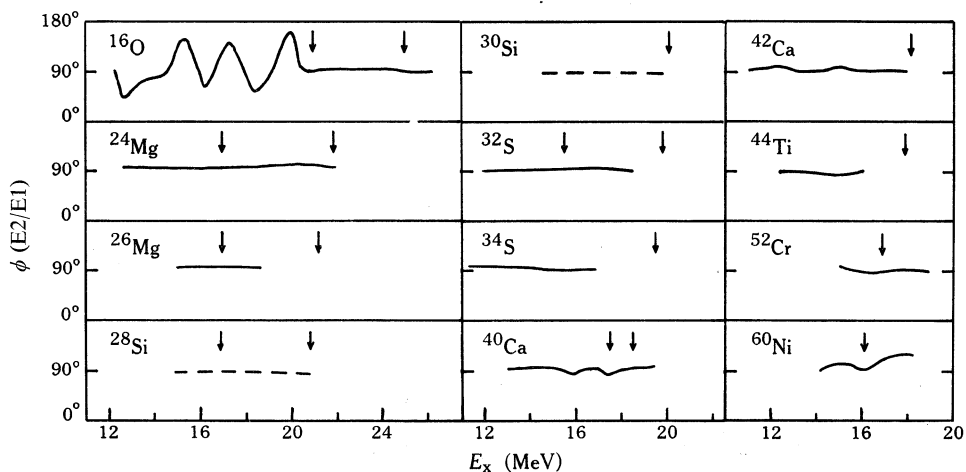


Fig. 22. Energy variation of E2, E1 relative phase angles in (α, γ) reactions. The arrows locate $63 A^{-1/3}$ MeV and 3 MeV below the E1 resonance. References may be found in Table 3.

(b) Polarized (p, γ_0) Reaction

The first evidence for E2 strength in the giant resonance region appeared when detailed angular distribution measurements became available in (p, γ) reactions (Allas *et al.* 1964a). The appearance of $P_3(\cos \theta)$ and in some cases $P_4(\cos \theta)$ terms in the angular distributions established the existence of E2 radiation interfering with the E1 resonance. Fig. 2d shows values of a_3 (the coefficient of P_3) measured (O'Connell *et al.* 1973) throughout the giant E1 resonance of ^{16}O . The values range between 0.1 and -0.2 . Unfortunately, if a_4 is too small to be measured reliably, as in this case, one cannot extract the E2 strength unambiguously from a_3 alone, because the E2–E1 phase difference is not known. However, if one is willing to make plausible assumptions about this phase difference, the E2 strength can be extracted (Frederick *et al.* 1969), as shown in Fig. 23 for the reaction $^{16}\text{O}(\gamma, p_0)^{15}\text{N}$. We observe the appearance of a giant E2 resonance between $E_x = 20$ and 33 MeV in ^{16}O , with perhaps evidence for two peaks. In several other nuclei from $A = 4$ to 40, E2 strength of this nature has been found in (p, γ) and (γ, p) measurements.

The breakthrough in these measurements came with the use of polarized protons in the (p, γ) measurements (Hanna *et al.* 1974). In a reaction such as the polarized reaction $^{15}\text{N}(p, \gamma)^{16}\text{O}$ where the spin of ^{15}N is $1/2$, specifying the proton spin makes it possible to remove the phase ambiguity and extract the E2 intensity from the polarized and unpolarized angular distributions. In order to obtain a reliable measure of the E2 intensity, it is necessary to make precise measurements of the angular distributions so as to extract accurate values of the coefficients in equations (1) and

(4) up to $k = 4$. The analysis is then expanded to include 2^+ resonances in ^{16}O and $p_{3/2}$ and $f_{5/2}$ waves in the reaction $^{15}\text{N}(p, \gamma_0)^{16}\text{O}$. We now have the following matrix elements in the entrance channel:

$$|s_{1/2}| \exp(i\phi_s), \quad |d_{3/2}| \exp(i\phi_d), \quad |p_{3/2}| \exp(i\phi_p), \quad |f_{5/2}| \exp(i\phi_f).$$

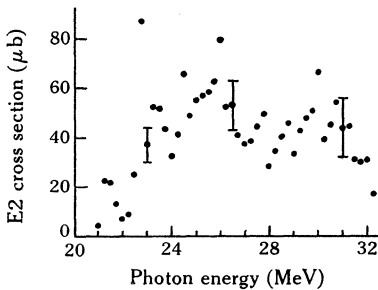


Fig. 23. Giant E2 resonance observed in $^{16}\text{O}(\gamma, p_0)^{15}\text{N}$ (Frederick *et al.* 1969).

The relationship between these quantities and the experimental coefficients can be expressed in terms of known functions

$$a_k = f_k(s_{1/2}, d_{3/2}, p_{3/2}, f_{5/2}, \phi_d - \phi_s, \phi_p - \phi_s, \phi_f - \phi_s), \quad k = 1 \rightarrow 4, \quad (14a)$$

$$b_k = g_k(s_{1/2}, d_{3/2}, p_{3/2}, f_{5/2}, \phi_d - \phi_s, \phi_p - \phi_s, \phi_f - \phi_s), \quad k = 1 \rightarrow 4, \quad (14b)$$

$$1 = 0.75(s_{1/2}^2 + d_{3/2}^2) + 1.25(p_{3/2}^2 + f_{5/2}^2), \quad (14c)$$

where the normalization condition has been appropriately modified. We now have nine equations and seven quantities to be determined (four amplitudes and three relative phases). However, for a complete solution it would be necessary to include M1 radiation in the analysis, which would introduce 1^+ resonances and $p_{1/2}$ and $p_{3/2}$ waves in $^{15}\text{N}(p, \gamma_0)^{16}\text{O}$. Fortunately, the M1 radiation can be effectively eliminated from the analysis by omitting the coefficients a_1 and b_1 from consideration. We are then left with seven equations and the seven unknown quantities describing the E1 and E2 strengths. Once these have been determined, it is then possible to insert the known E1 and E2 parameters into the equations for a_1 and a_2 to test for the presence of M1 radiation. In the measurements made so far in the giant E1 regions of several nuclei, the M1 contributions have been found to be very small.

Some typical angular distributions for $^{15}\text{N}(p, \gamma_0)^{16}\text{O}$ are shown in Fig. 24. These measurements illustrate the quality of the data which can be achieved by careful measurements in relatively short periods of time. On the basis of such measurements, carried out between $E_x = 19$ and 28 MeV and shown in Fig. 25, the $p_{3/2}$ and $f_{5/2}$ amplitudes and phases were extracted from the equations (14), and the total E2 cross sections were obtained as shown in Fig. 26. Although there are still two solutions (I and II), it is a fortunate circumstance that both solutions lead to essentially the same E2 cross sections. Although the absolute cross section differs a little, the shape of the E2 resonance in Fig. 23 agrees quite well with the E2 resonance in Fig. 26e.

In Fig. 27 we see collected together all the E2 strength in ^{16}O determined by γ -ray reactions, taken from Figs 21a and 26e with the latter curve extended to higher energy by unpolarized (p, γ) work from Brookhaven (P. Paul, personal communication). As we expect to find strength in the n_0 channel comparable with that in the p_0

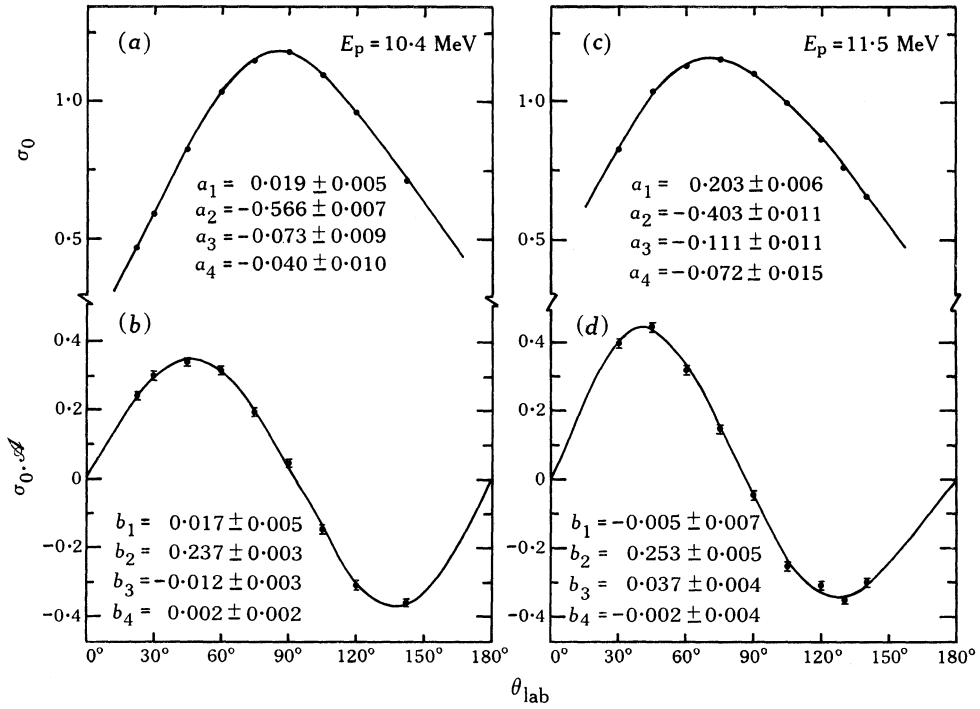


Fig. 24. Unpolarized (a and c) and polarized (b and d) angular distributions from $^{15}\text{N}(p, \gamma_0)^{16}\text{O}$ at $E_p = 10.4$ and 11.5 MeV.

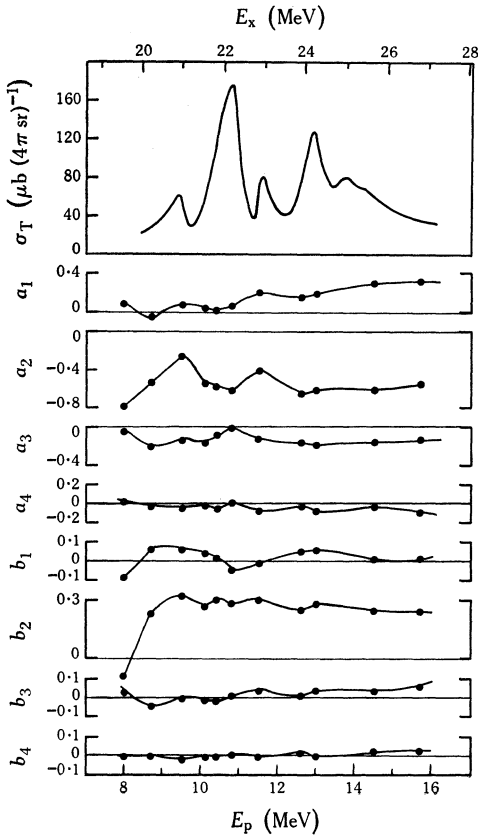


Fig. 25. Total cross section σ_T and unpolarized and polarized coefficients a_k and b_k ($k = 1, \dots, 4$) for $^{15}\text{N}(p, \gamma_0)^{16}\text{O}$.

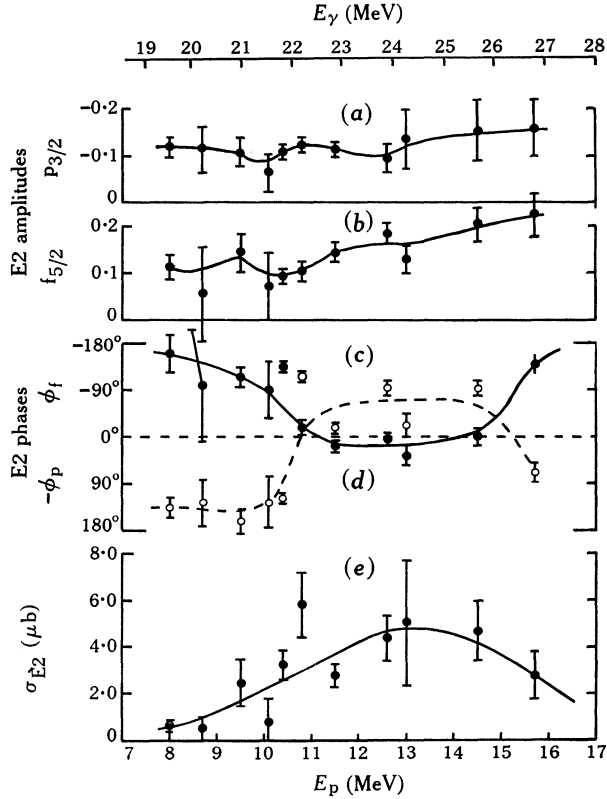


Fig. 26. E2 amplitudes, phases and cross section derived from the coefficients given in Fig. 25 for the polarized reaction $^{15}\text{N}(p, \gamma_0)^{16}\text{O}$.

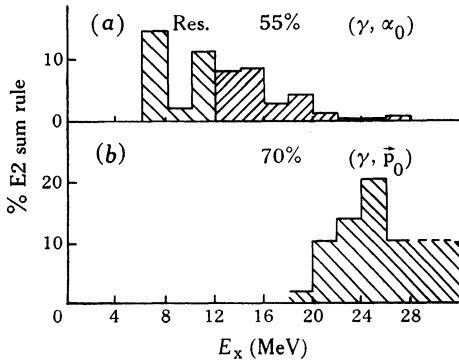


Fig. 27. Summary of E2 strength in ^{16}O from γ -ray reactions.

channel, the total yield represented by Fig. 27 probably greatly exceeds the isoscalar E2 sum rule. Clearly, a considerable portion of the strength must be isovector in character.

But how is the isoscalar and isovector strength to be divided up, if indeed it can be separated at all? One way would be to assign the strength shown in Fig. 27a principally to $T = 0$ and that shown in Fig. 27b to $T = 1$. If the unobserved strength in both regions is taken into account (with some of the p_0 strength around $E_x = 20 \rightarrow 24$ MeV identified as $T = 0$), this assignment would satisfy nicely both the

isoscalar and isovector sum rules. It would agree as well with the identification of a substantial part of the (γ, p_0) strength with $T = 1$ on the basis of a comparison of the signs of the odd Legendre coefficients in the (γ, p_0) and (γ, n_0) angular distributions (Snover *et al.* 1974a). However, this identification of isospin splitting would not agree well with the theoretical calculations. In Figs 28 and 29 are given the results of two

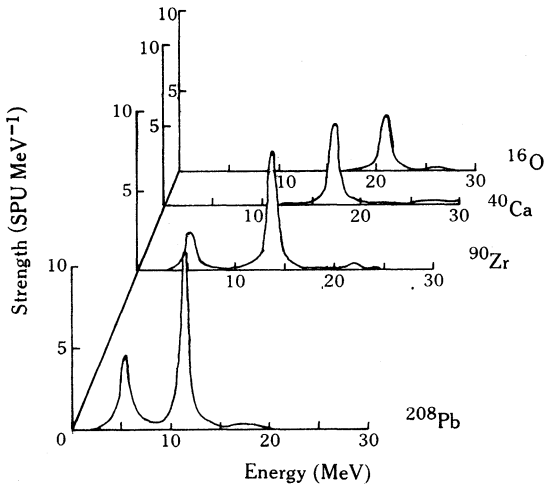


Fig. 28. Isoscalar E2 strength (SkI) computed for ^{16}O , ^{40}Ca , ^{90}Zr and ^{208}Pb (Bertsch and Tsai 1975).

calculations (Krewald *et al.* 1974, and S. Krewald, personal communication; Bertsch and Tsai 1975) of the E2 strength based on $1p-1h$ excitations of $2\hbar\omega$ type (see Fig. 19). Both calculations place the major isoscalar strength in a compact peak at about 22 MeV, which would agree rather well with the resonance seen in (γ, p_0) shown in Figs 26e and 27b. However, the other E2 strength spread out over lower excitation

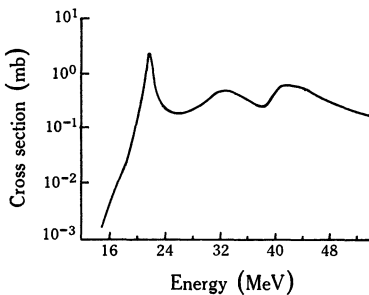


Fig. 29. Isoscalar and isovector E2 strength computed for ^{16}O (Krewald *et al.* 1974).

energies (Fig. 27a) is of course also isoscalar and would have to be assigned to more complex excitations, such as $2p-2h$ (see Fig. 19), $4p-4h$, etc. Indeed, several earlier calculations of the E2 strength in ^{16}O which included $2p-2h$ excitations show a very pronounced spreading downward of the E2 levels. The results of one such calculation (Philpott and Szydlík 1967) are given in Fig. 30. In addition, it seems very reasonable that $1p-1h$ excitations should give rise to (γ, p_0) yield and that more complex excitations should give rise to (γ, α_0) decay.

However, if all this strength is assigned as isoscalar E2, it would undoubtedly greatly exceed the sum rule. Hence, much of the strength in the region above 22 MeV would have to be isovector, and the isospin in this region might be quite thoroughly mixed. The observed extension of the strength to higher energies (Frederick *et al.* 1969; Peschel *et al.* 1974) (see dashed line in Fig. 27b) could still be predominantly isovector and would agree with the calculated cross section shown in Fig. 29. Experimentally, at present, it is not possible to decide between these two pictures of the isospin splitting. In either case the isoscalar E2 strength in ^{16}O is spread over a wide region from about 6 MeV to some energy between 20 and 30 MeV.

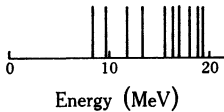


Fig. 30. 2^+ , $T = 0$ levels in ^{16}O computed with 1p-1h and 2p-2h excitations (Philpott and Szydlik 1967).

Based on the evidence of Fig. 21 we might expect the same picture as observed in ^{16}O to hold up to ^{40}Ca , if not beyond. This is confirmed by γ -ray measurements in ^{24}Mg (Fig. 31) and ^{32}S (Fig. 32). In ^{24}Mg the E2 strength found by γ -ray spectroscopy in the bound levels (Endt and Van der Leun 1973) together with the α_0 strength (see 1974 Stanford Progress Report; Kuhlmann *et al.* 1975) is compared with the strength observed by a detailed high-resolution study (Singh and Yang 1974) of $^{24}\text{Mg}(\alpha, \alpha')$.

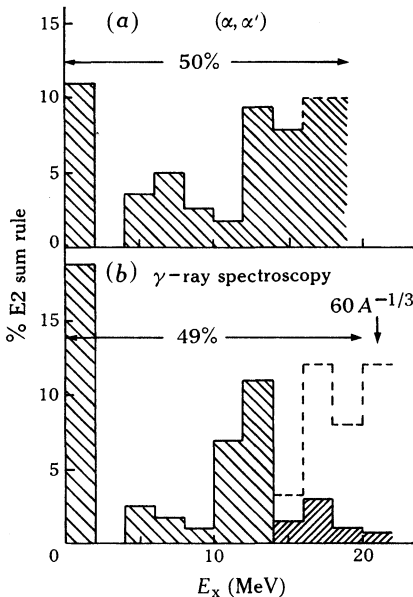


Fig. 31. Comparison of isoscalar E2 strength in ^{24}Mg from (a) inelastic α -particle excitation (Singh and Yang 1974) with that from (b) γ -ray reactions.

If a plausible correction for missing strength in other channels is made (dashed line in Fig. 31b), the two distributions are in qualitative agreement and account for about 50% (α, α') or 70% (γ -ray spectroscopy) of the isoscalar E2 sum rule. In ^{32}S (Fig. 32) the picture is very similar to ^{16}O except that the (γ, p_0) and (γ, α_0) strengths (see 1974 Stanford Progress Report; Kuhlmann *et al.* 1975) overlap more, and the (γ, p_0) strength, in agreement with a $63 A^{-1/3}$ law, coincides with the E1 resonance (while in ^{16}O it is somewhat above).

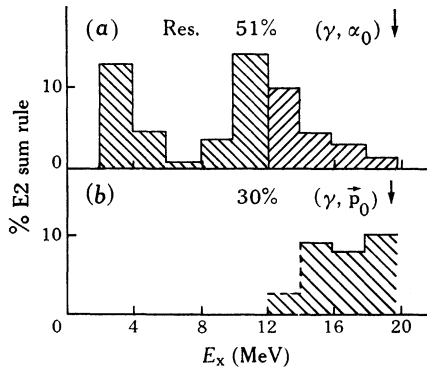


Fig. 32. Summary of E2 strength in ^{32}S from γ -ray reactions.

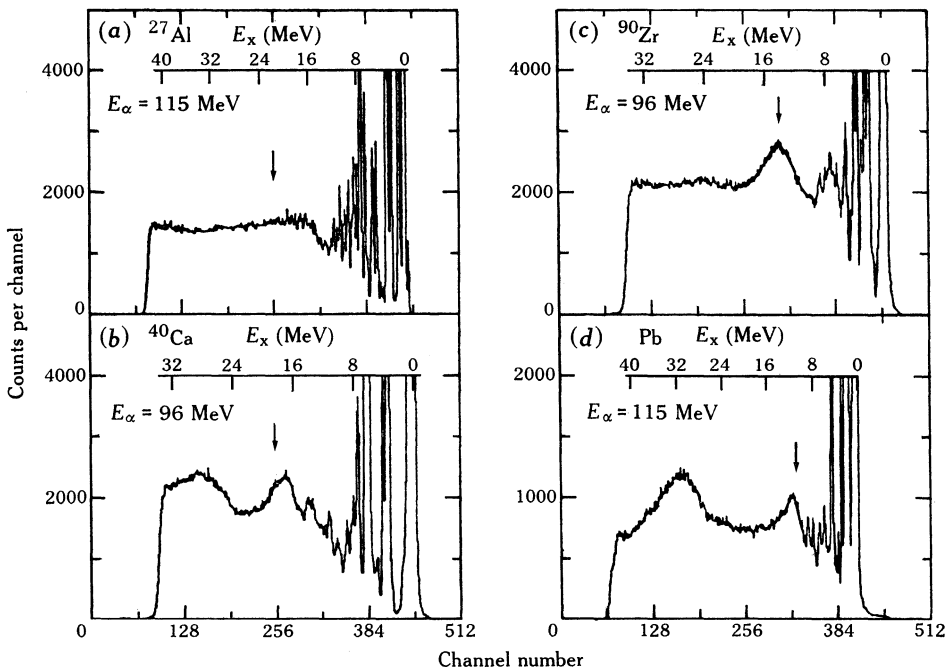


Fig. 33. Inelastic α -particle excitations of ^{27}Al , ^{40}Ca , ^{90}Zr and Pb (Moss *et al.* 1975).

(c) Inelastic Scattering

What is the evidence that can be obtained from inelastic excitation? The early work (Lewis and Bertrand 1972; Bertrand *et al.* 1973) on (p, p') indicated a compact isoscalar resonance lying below the E1 resonance down to at least ^{27}Al . Such a resonance in ^{27}Al would be difficult to reconcile with the evidence presented above. The recent work (see 1974 Texas A&M Progress Report; Moss *et al.* 1975) on (α, α') has greatly clarified the picture. The α -particle reaction has the great advantage of selectively exciting isoscalar electric multipoles only.

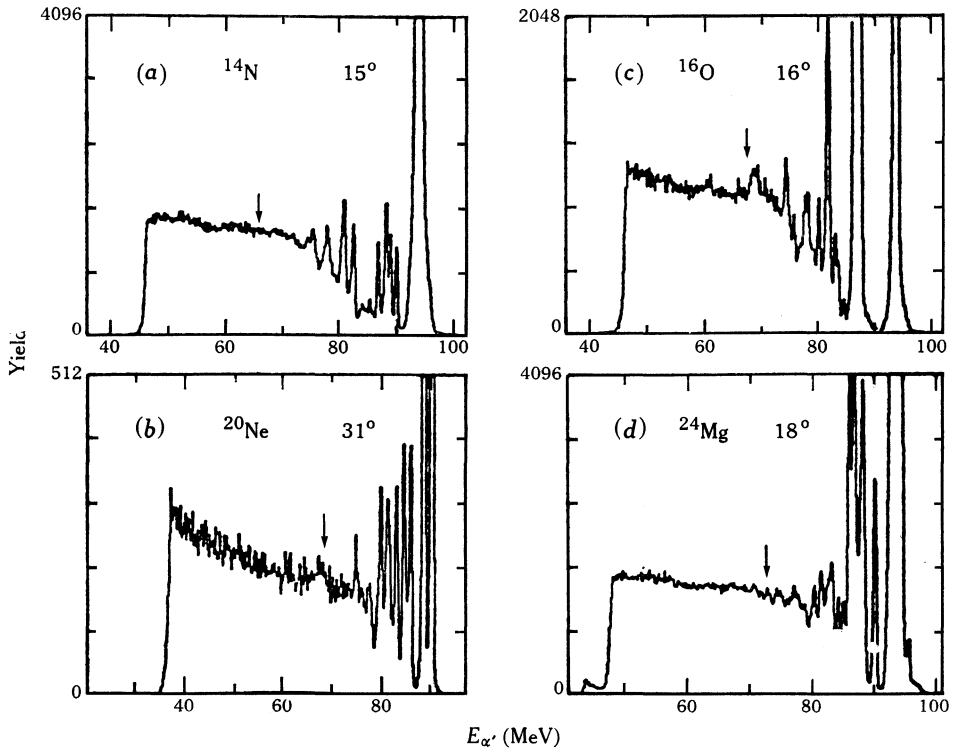


Fig. 34. Inelastic α -particle excitation of ^{14}N , ^{20}Ne , ^{16}O and ^{24}Mg (Moss *et al.* 1975).

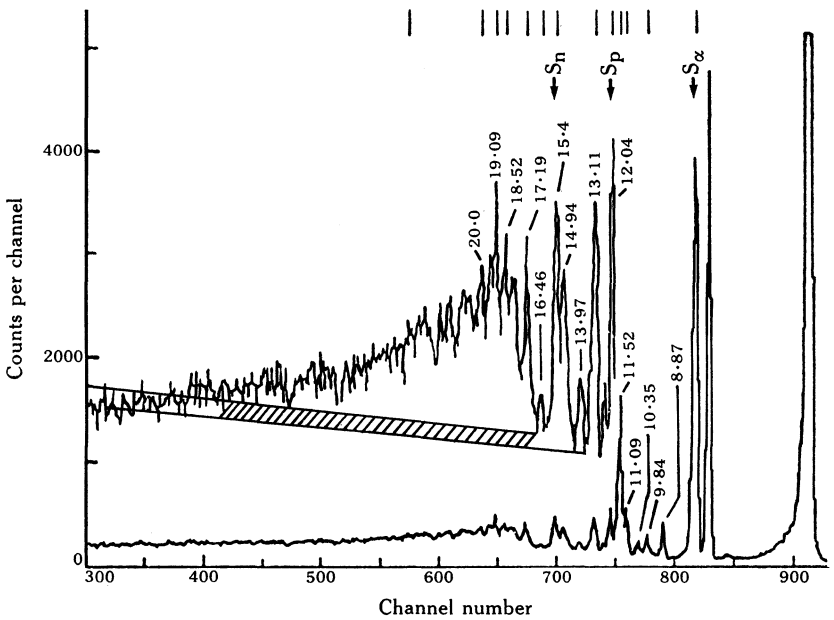
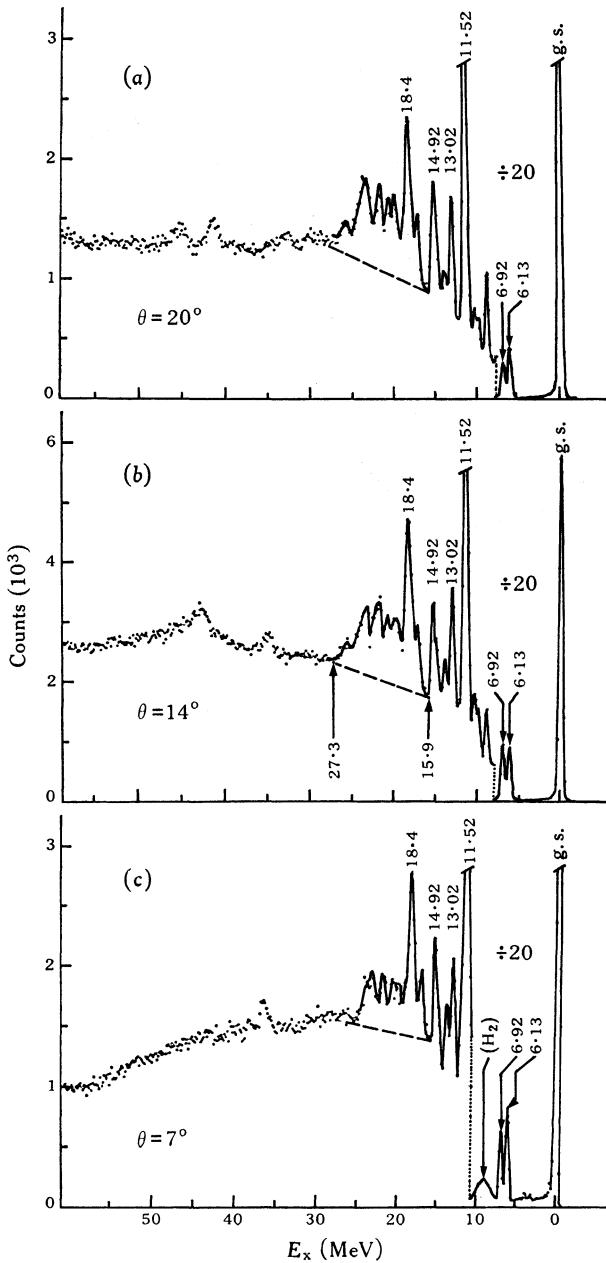


Fig. 35. Inelastic ^3He excitation of ^{16}O for ^3He energy of 71 MeV and $\theta_{\text{lab}} = 20^\circ$ (Moalem *et al.* 1974).



Figs 36a–36c. Inelastic α -particle excitation of ^{16}O at three selected angles (Knöpfle *et al.* 1975).

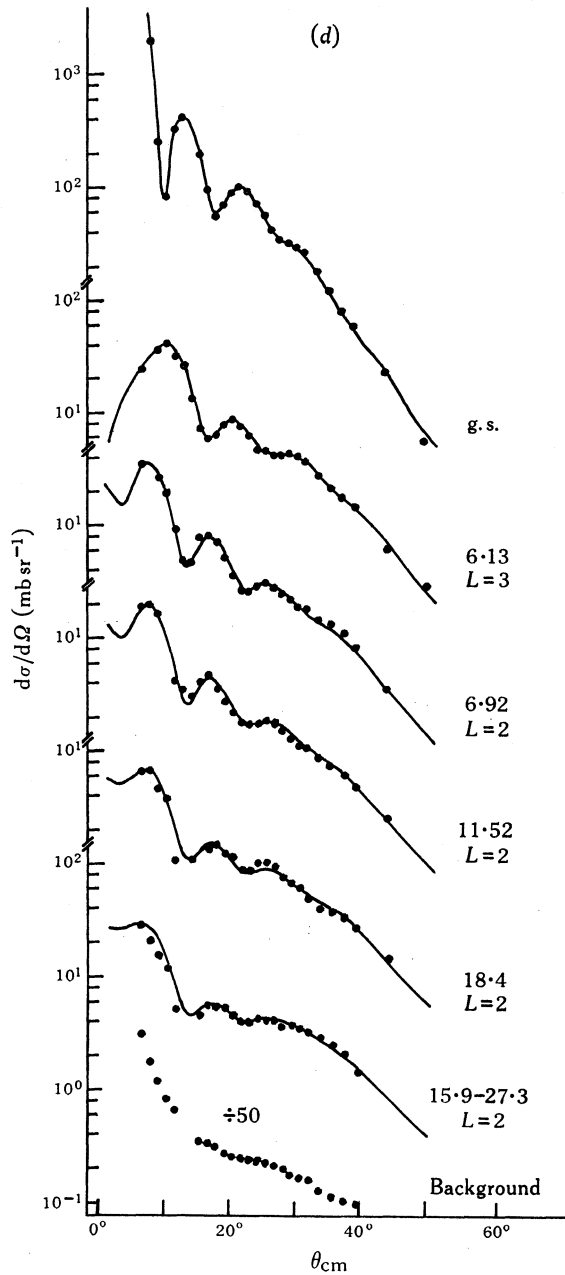


Fig. 36d. Angular distributions of 2^+ resonances from inelastic α -particle excitation of ^{16}O for $E_x = 146$ MeV (Knöpfle *et al.* 1975).

In Figs 33b–33d we see a compact isoscalar resonance at $63A^{-1/3}$ in ^{40}Ca , ^{90}Zr and Pb , but in ^{27}Al (Fig. 33a) the resonance has washed out into a broad shoulder indicative of a spreading out of the strength. This picture is maintained throughout the light nuclei as shown for ^{14}N , ^{16}O , ^{20}Ne , and ^{24}Mg in Figs 34a–34d. The authors of this work (1974 Texas A&M Progress Report; Moss *et al.* 1975) did not attempt to draw a background under this shoulder in order to extract an E2 strength. It would appear that the evidence from (α, α') given in Figs 33 and 34 is qualitatively compatible with the evidence from γ -ray reactions presented in Figs 21, 27, 31 and 32.

Results from $^{16}\text{O}(^3\text{He}, ^3\text{He}')$ (Moalem *et al.* 1974) are presented in Fig. 35. This reaction is much more sensitive to isoscalar E2 strength than to isovector strength. We see that the main concentration of isoscalar strength lies in the 16 to 26 MeV region, with strong peaking at 19 MeV. Thus, this isoscalar strength lies definitely below the strength seen in the polarized (p, γ_0) reaction (Figs 26 and 27) and supports the conclusion that the latter strength is largely isovector in nature.

Still more recently, the isoscalar E2 strength has been displayed (Knöpfle *et al.* 1975) rather convincingly in (α, α') measurements at high energy ($E_\alpha = 146$ MeV). The result is shown in Fig. 36. That the strength above the dashed line in Figs 36a–36c is predominantly E2 is established by the angular distributions (Fig. 36d). Although differing in detail, the isoscalar strength from (α, α') agrees in its main features very nicely with the result from $(^3\text{He}, ^3\text{He}')$ and appears to establish that the main concentration of isoscalar E2 strength in ^{16}O is centered at about 19 to 20 MeV. This lowering of the isoscalar strength is indicated by the dotted line in Fig. 1.

Recently, electron scattering measurements (Hotta *et al.* 1974) have also confirmed the results of the γ -ray measurements on ^{16}O . In particular, the results show 43% of the E2 sum rule below 20 MeV and only 20% between 20 and 30 MeV.

We now come to ^{40}Ca which could prove to be the pivotal case between the light and heavy nuclei. Fig. 37 shows the results (Torizuka *et al.* 1973) of inelastic electron excitation on ^{40}Ca . A background has been subtracted and a semi-empirical technique has been used to sort out the various multipoles. Actually it is not possible to distinguish E2 from E0. Thus, we see that the E2(E0) strength is rather uniformly spread between 10 and 20 MeV, in rather good agreement with the picture developed above for E2 strength in the lighter nuclei. Since the 1p–1h calculations (see Fig. 28) place the isoscalar E2 strength in a compact resonance at 17 MeV, an attempt was made (Hammerstein *et al.* 1974) to divide the E2(E0) strength in Fig. 37 into an E2 resonance at 17.5 MeV and an E0 resonance at 14 MeV as shown in Fig. 38. This assignment of E0 strength is doubtful for at least three reasons:

(1) This strength in the region of 14 MeV, which appears in both (e, e') and (α, α') is probably seen strongly in (γ, α_0) , as shown by the comparison in Fig. 39. Since E0 strength cannot be excited by γ -rays, the yield in this region is very probably E2.

(2) Preliminary results from particle–particle angular correlation measurements (A. Moalem, personal communication) indicate that the correlation throughout the region between 10 and 20 MeV is not isotropic. This result would rule out any major strength in spin-0 resonances.

(3) The theoretical calculations (Krewald *et al.* 1974; S. Krewald, personal communication; Bertsch and Tsai 1975) place the major E0 strength at about 24 MeV as shown in Fig. 40.

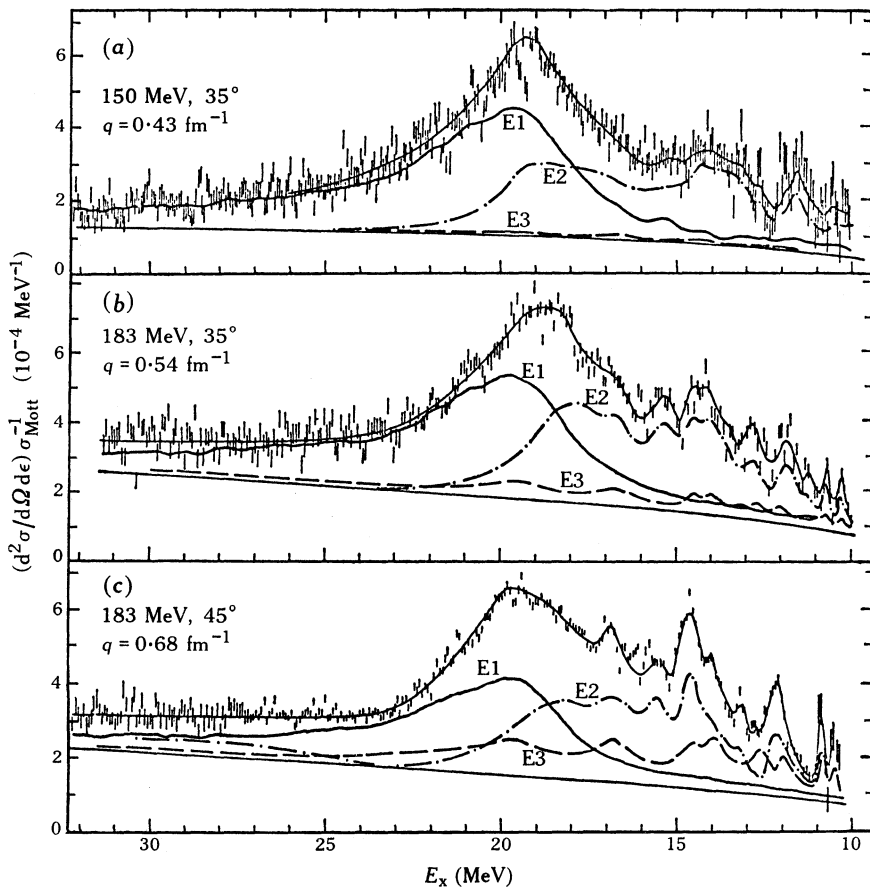


Fig. 37. Inelastic electron excitation of ^{40}Ca at different momentum transfers (Torizuka *et al.* 1973).

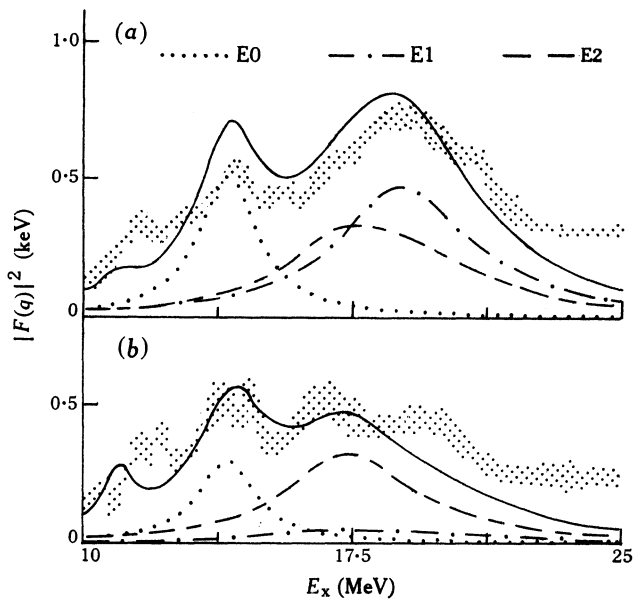


Fig. 38. Suggested assignment of multipole strength from $^{40}\text{Ca}(e, e')$ (Hammerstein *et al.* 1974).

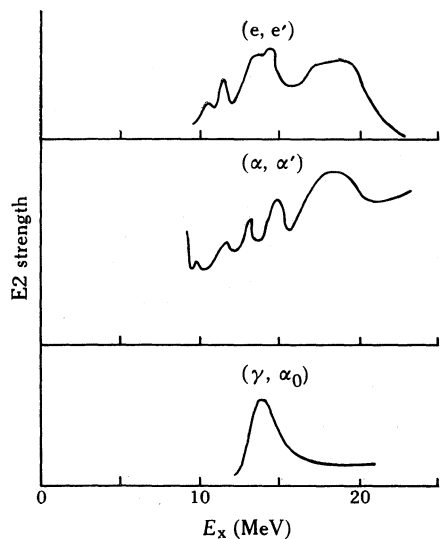


Fig. 39. Comparison of E2 strength in ^{40}Ca from the three indicated reactions.

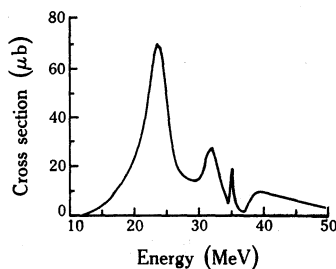


Fig. 40. Breathing mode calculated for ^{40}Ca (Krewald *et al.* 1974).

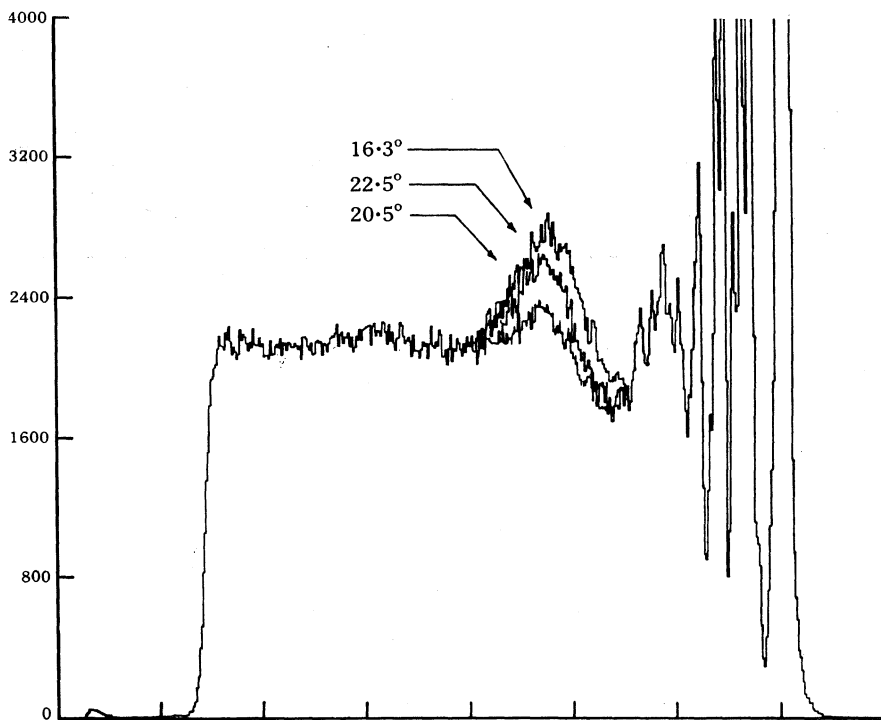


Fig. 41. Inelastic α -particle excitation of ^{90}Zr at three selected angles (Moss *et al.* 1975).

In the heavier nuclei the isoscalar E2 resonances have been the subject of many papers and several reviews; e.g. see the review of Walcher (1973) presented at Munich. The analysis of these resonances has been based on the extensive work of Satchler (1972, 1973). No attempt is made here to review the complete picture, but instead a few significant, recent developments are presented.

By means of the (α, α') reaction, which selectively excites isoscalar strength, the Texas A&M group has obtained definitive angular distributions in a number of cases (see their 1974 Progress Report; Moss *et al.* 1975). The results given in Fig. 41 on ^{90}Zr show convincingly the existence of a compact isoscalar resonance at $63 A^{-1/3}$, with an angular distribution which oscillates in phase with an E2 distribution and exhausts 54% of the E2 sum rule.

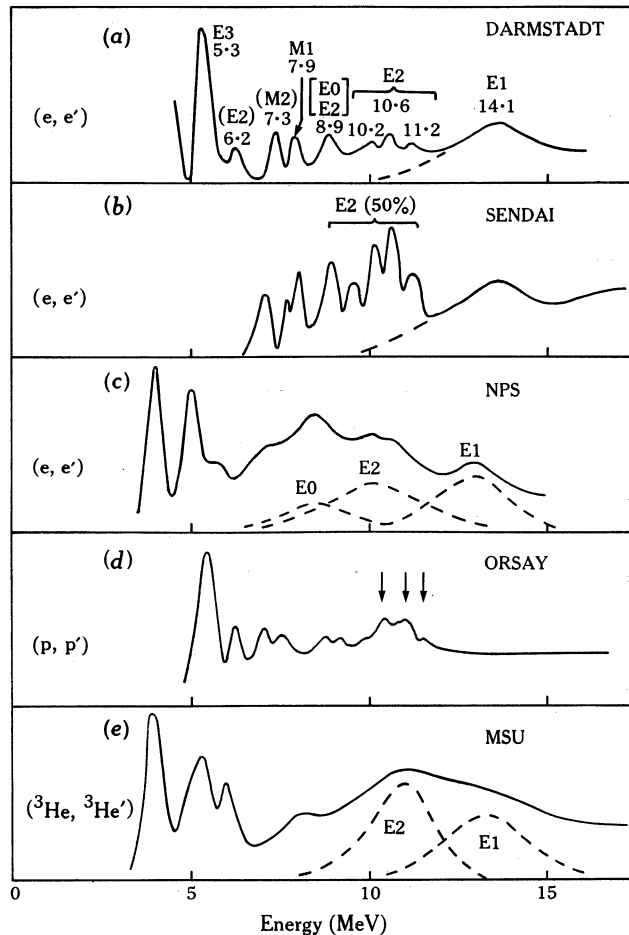


Fig. 42. Comparison between results obtained from inelastic excitation of ^{208}Pb by (a) Walcher (1973), (b) Nagao and Torizuka (1973), (c) Buskirk *et al.* (1974), (d) Marty *et al.* (1975), (e) Moalem *et al.* (1973).

Many spectra have been obtained on ^{208}Pb . Figs 42 and 43 are an attempt to compare some of them. It is clear that with good resolution a great deal of structure is present in ^{208}Pb . The three peaks at 10.1, 10.6, and 11.4 MeV, seen in (p, p') and (e, e') are reported (Walcher 1973) as E2, as is the structure at 6.2 MeV (Ziegler and Peterson 1968). Thus, the spreading of the E2 strength in Pb may be quite appreciable. The structure at 8.9 MeV could well be E2 but it has been argued (Buskirk *et al.* 1974; R. Pitthan, personal communication) that this resonance is E0 on the basis that it is not observed in the (γ, n) yield, while the higher E2 resonances are probably

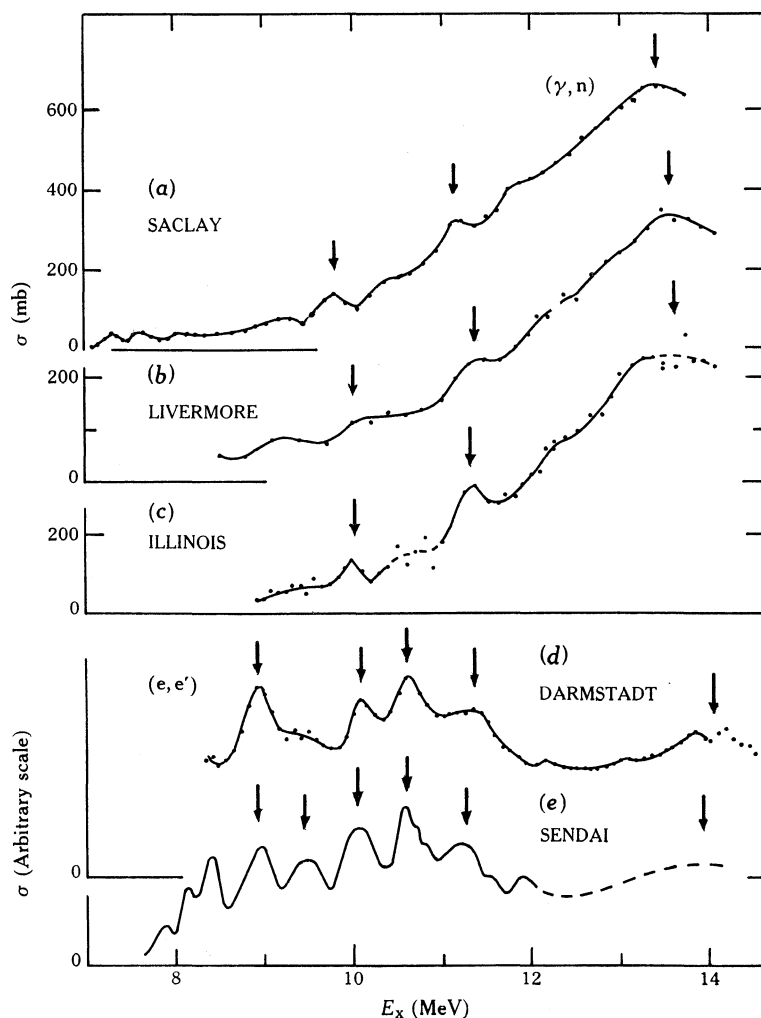


Fig. 43. Comparison between results obtained from photonuclear excitation with monoenergetic photons and from high-resolution inelastic electron scattering by (a) Veysière *et al.* (1970), (b) Berman and Fultz (1975), (c) Young (1972), (d) Walcher (1973), (e) Nagao and Torizuka (1973).

seen as small wiggles on the dominant E1 cross section (see below). However, as was the case for ^{40}Ca discussed above, the calculations (Krewald *et al.* 1974; Bertsch and Tsai 1975) place the monopole strength at 20 MeV or above. The calculation of the E2 strength in ^{208}Pb , shown in Fig. 28, gives major strength at 5 MeV and in the 11 to 15 MeV (depending on the interaction) region, in rather good agreement with experiment, but reveals no strength at 9 MeV.

In view of the above arguments, it is instructive to compare the (e, e') results (Veysière *et al.* 1970; Young 1972; Berman and Fultz 1975, who reproduced Young's data) with the (γ , n) measurements made with monochromatic photons, as is done in Fig. 43. The agreement among the (γ , n) curves is quite good, provided the Saclay result is shifted in energy by about 200 keV. It is seen that the two peaks, at 10.1

and 11.4 MeV, are quite well established in these curves. The strengths of these peaks are compatible with E2 radiation, and coincide with the peaks seen in (e, e'). There is less evidence for the peaks at 10.6 and 8.9 MeV, and the assignment of these peaks as E2 should not be considered as established at present. On the other hand, it has been recently shown (Schwierczinski *et al.* 1975) that the strength of the (e, e') peak at 8.9 MeV is compatible with the (γ , n) curves, so that it is not necessary to assign this peak to E0. Clearly, the Pb isotopes require further detailed study.

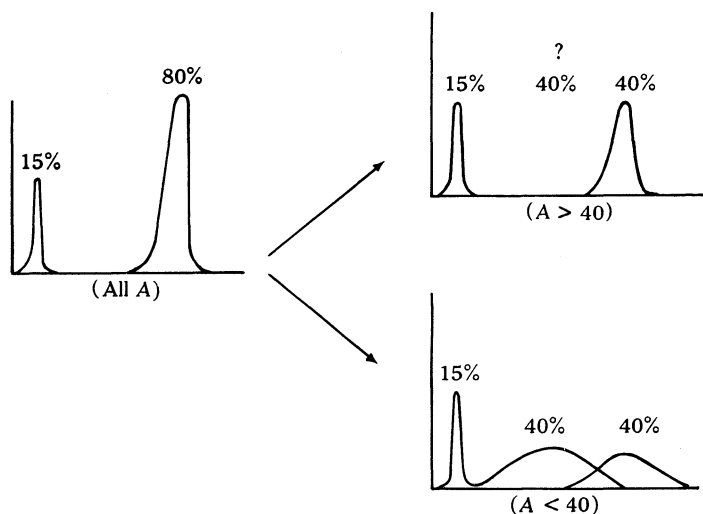


Fig. 44. Schematic distribution of isoscalar E2 strength a year ago and now [1975].

Table 4. Parameters of E1 resonances from (p, p') at 155 MeV

| Nucleus | $EA^{1/3}$ (MeV) | Γ (MeV) | % S.R. | Nucleus | $EA^{1/3}$ (MeV) | Γ (MeV) | % S.R. |
|-------------------|---------------------|-------------------|--------|-------------------|---------------------|-------------------|--------|
| ⁴⁰ Ca | 63 | | 49 | ¹⁸¹ Ta | 63 | 3.9 | 42 |
| Fe | 62 | (5.1) | 37 | ¹⁹⁷ Au | 63 | 2.5 | 36 |
| ⁸⁹ Y | 62 | 3.2 | 24 | ²⁰⁸ Pb | 64 | 2.2 | 28 |
| ¹¹⁵ In | 64 | 3.5 | 14 | | 55 | | 11 |
| Sn | 63 | 3.3 | 17 | ²⁰⁹ Bi | 64 | 2.2 | 29 |
| ¹⁶⁵ Ho | 64 | 3.6 | (26) | | 53 | | 9 |

As noted above, many values for the strengths of the compact isoscalar E2 resonances have been reported. Table 4 reproduces a recent tabulation of results from inelastic proton scattering (Marty *et al.* 1975) which shows variations between 14% and 49% of the isoscalar E2 sum rule. Although other measurements from (p, p'), (d, d'), (³He, ³He'), (α , α') and (e, e') may disagree with individual values in Table 4, they nevertheless agree in showing a wide range of values. A reasonable average of all the results is something like 40%.

The E2 giant resonances have also been studied through the contribution they make to other inelastic processes (Amos and Geramb 1974) and to effective charges (Blomqvist 1973; A. Arima, personal communication). In addition to the $T = 1$ strength in ¹⁶O discussed above, evidence has been accumulating on the isovector

giant E2 resonance in many nuclei (Urbas and Greiner 1970; Klawansky *et al.* 1973; Nagao and Torizuka 1973; Walcher 1973; Snover *et al.* 1974b) at a position of about $124 A^{-1/3}$.

We may summarize the status of the isoscalar E2 strength very schematically by Fig. 44. The picture that existed at the Munich meeting (Walcher 1973) is shown on the left; the situation which emerges today is on the right. It should be added that in the heavier nuclei the 'missing' E2 strength may turn up in the compact E2 resonance when better measurements are available, or it may be found to be distributed over complex configurations as appears to be the case in the light nuclei. Hopefully, another year will settle this question.

For the M1 levels the important problems are to obtain the complete strength in key nuclei such as Pb, and to make a systematic study of the strength and spreading, especially in the heavy nuclei. For the E2 resonances the important problems are to obtain definitive strengths, to locate all the strength, to determine the isospin of the resonances and their decay modes (including angular correlations) and to include more complex configurations in the theory.

Acknowledgments

It is a pleasure to acknowledge my colleagues who have participated in the research at Stanford reported here. The experiments were carried out in collaboration with J. R. Calarco, G. A. Fisher, H. F. Glavish, G. King, E. Kuhlmann, R. LaCanna and D. G. Mavis. The calculations on the E1 resonance of ^{16}O are due to H. F. Glavish and D. G. Mavis.

References

- Ajzenberg-Selove, F. (1970). *Nucl. Phys. A* **152**, 1.
 Ajzenberg-Selove, F. (1971). *Nucl. Phys. A* **166**, 1.
 Ajzenberg-Selove, F. (1972). *Nucl. Phys. A* **190**, 1.
 Ajzenberg-Selove, F. (1975). *Nucl. Phys. A* **248**, 1.
 Ajzenberg-Selove, F., and Lauritsen, T. (1974). *Nucl. Phys. A* **227**, 1.
 Allas, R. G., Hanna, S. S., Meyer-Schützmeister, L., and Segel, R. E. (1964a). *Nucl. Phys.* **58**, 122.
 Allas, R. G., Hanna, S. S., Meyer-Schützmeister, L., Segel, R. E., Singh, P. P., and Vager, Z. (1964b). *Phys. Rev. Lett.* **13**, 187.
 Amos, K., and Geramb, H. V. (1974). Proc. Int. Conf. on Nuclear Structure and Spectroscopy, Amsterdam (Eds H. P. Blok and A. E. L. Dieperink), Vol. 1, p. 160 (Scholar's Press: Amsterdam).
 Axel, P., Drake, D. M., Whetstone, S., and Hanna, S. S. (1967). *Phys. Rev. Lett.* **19**, 1343.
 Barber, W. C. (1962). *Annu. Rev. Nucl. Sci.* **12**, 1.
 Barber, W. C., Goldemberg, J., Peterson, G. A., and Torizuka, Y. (1963). *Nucl. Phys.* **41**, 461.
 Barit, I. Ya., and Sergejev, V. A. (1967). *Sov. J. Nucl. Phys.* **4**, 1507.
 Bartholomew, G. A., Earle, E. D., Ferguson, A. J., Knowles, J. W., and Lone, M. A. (1973). In 'Advances in Nuclear Physics' (Eds M. Baranger and E. Vogt), Vol. 7, p. 229 (Plenum: New York).
 Berman, B. L., and Fultz, S. C. (1975). *Rev. Mod. Phys.* **47**, 713.
 Bertozzi, W., *et al.* (1964). Cong. Int. Physique Nucléaire (Ed. P. Gugenberger), Vol. 2, p. 1026 (Centre National de la Recherche Scientifique: Paris).
 Bertrand, F. E., Gross, E. E., Horen, D. J., Kocher, D. C., Lewis, M. B., and Newman, E. (1973). Annual Report of the Physics Division, ORNL.
 Bertsch, G. F., and Tsai, S. F. (1975). *Phys. Rep. C* **18**, 125.
 Black, J. L., O'Connell, W. J., Hanna, S. S., and Latshaw, G. L. (1967). *Phys. Lett. B* **25**, 405.
 Blomqvist, J. (1973). *J. Phys. Soc. Jpn* **34** (Suppl.).
 Bohr, A., and Mottelson, B. R. (1975). 'Nuclear Structure', Vol. 2 (Benjamin: New York).
 Bollinger, L. M. (1973). Proc. Int. Conf. on Photonuclear Reactions and Applications, Asilomar (Ed. B. L. Berman), Vol. 2, p. 783 (USAEC Office of Information Services: Oak Ridge).

- Bollinger, L. M., and Thomas, G. E. (1970). *Phys. Rev. C* **2**, 1951.
- Bowman, C. D., Baglan, R. J., Berman, B. L., and Phillips, T. W. (1970). *Phys. Rev. Lett.* **25**, 1302.
- Brown, G. E., Castillejo, L., and Evans, J. A. (1961). *Nucl. Phys.* **22**, 1.
- Buskirk, F. R., *et al.* (1973). Proc. Int. Conf. on Photonuclear Reactions and Applications, Asilomar (Ed. B. L. Berman), Vol. 1, p. 703 (USAEC Office of Information Services: Oak Ridge).
- Buskirk, F. R., *et al.* (1974). Proc. Int. Conf. on Nuclear Structure and Spectroscopy, Amsterdam (Eds H. P. Blok and A. E. L. Dieperink), Vol. 1, p. 205 (Scholar's Press: Amsterdam).
- Cecil, F. E., Kuo, T. T. S., and Tsai, S. F. (1973). *Phys. Lett. B* **45**, 217.
- Chang, C. C., Bertrand, F. E., and Kocher, D. C. (1975). *Phys. Rev. Lett.* **34**, 221.
- Cohen, D., Moyer, B. J., Shaw, H., and Waddell, C. (1954). *Phys. Rev.* **96**, 714.
- Cohen, L., and Tobin, R. A. (1959). *Nucl. Phys.* **14**, 243.
- Crone, L., and Wernitz, C. (1969). *Nucl. Phys. A* **134**, 161.
- Earle, E. D., and Tanner, N. W. (1967). *Nucl. Phys. A* **95**, 241.
- Edge, R. D., and Peterson, G. A. (1962). *Phys. Rev.* **128**, 2750.
- Ejiri, H., and Bondorf, J. (1968). *Phys. Lett. B* **28**, 304.
- Elliot, J. P., and Flowers, B. H. (1957). *Proc. R. Soc. London A* **242**, 57.
- Endt, P. M., and Van der Leun, C. (1973). *Nucl. Phys. A* **214**, 1.
- Fagg, L. W. (1973). Proc. Int. Conf. on Photonuclear Reactions and Applications, Asilomar (Ed. B. L. Berman), Vol. 1, p. 663 (USAEC Office of Information Services: Oak Ridge).
- Fagg, L. W. (1975). *Rev. Mod. Phys.* **47**, 683.
- Fagg, L. W., Bendel, W. L., Jones, E. C., Jr, Ensslin, N., and Cecil, F. E. (1973). Proc. Int. Conf. on Nuclear Physics, Munich (Eds J. de Boer and H. J. Mang), Vol. 1, p. 631 (North-Holland: Amsterdam).
- Fallieros, S., Goulard, B., and Venter, R. H. (1965). *Phys. Lett.* **19**, 398.
- Feshbach, H., Kerman, A. K., and Lemmer, R. H. (1967). *Ann Phys. (New York)* **41**, 230.
- Foote, G. S. (1974). Ph.D. Thesis, Australian National University.
- Frederick, D. E., Stewart, R. J. J., and Morrison, R. C. (1969). *Phys. Rev.* **186**, 992.
- Fuller, E. G., *et al.* (1973). 'Photonuclear Reaction Data', Nat. Bur. Stand. (U.S.) Spec. Publ. p. 380.
- Gillet, V., Melkanoff, M. A., and Raynall, J. (1967). *Nucl. Phys. A* **97**, 631.
- Gillet, V., and Vinh-Mau, N. (1964). *Nucl. Phys.* **54**, 321.
- Glavish, H. F. (1971). Proc. 3rd Int. Symp. on Polarization Phenomena in Nuclear Reactions, Madison (Eds H. H. Barschall and W. Haeblerli), p. 267 (Univ. Wisconsin Press: Madison).
- Gove, H. E., Purser, K. H., Schwartz, J. J., Alford, W. P., and Cline, D. (1968). *Nucl. Phys. A* **116**, 369.
- Hafstad, L. R., Heydenburg, N. P., and Tuve, M. A. (1936). *Phys. Rev.* **50**, 504.
- Hammerstein, G. R., McManus, H., Moalem, A., and Kuo, T. T. S. (1974). *Phys. Lett. B* **49**, 235.
- Hanna, S. S. (1969a). In 'Isospin in Nuclear Physics' (Ed. D. H. Wilkinson), Ch. 12, p. 592 (North-Holland: Amsterdam).
- Hanna, S. S. (1969b). In 'Nuclear Isospin' (Eds J. D. Anderson, S. D. Bloom, J. Cerny and W. W. True), p. 18 (Academic: New York).
- Hanna, S. S. (1974). Proc. 6th Masurian School in Nuclear Physics, Mikołajki, Nukleonika, Vol. 19 (7-8) pp. 655.
- Hanna, S. S., Glavish, H. F., Avida, R., Calarco, J. R., Kuhlmann, E., and LaCanna, R. (1974). *Phys. Rev. Lett.* **32**, 114.
- Harakeh, M., Paul, P., and Snover, K. A. (1975). *Phys. Rev. C* **11**, 998.
- Hardekopf, R. A., Lisowski, P. W., Rhea, T. C., Walter, R. L., and Clegg, T. B. (1972). *Nucl. Phys. A* **191**, 481.
- Hasinoff, M., Fisher, G. A., and Hanna, S. S. (1973). *Nucl. Phys. A* **216**, 221.
- Hasinoff, M., Fisher, G. A., Kuan, H. M., and Hanna, S. S. (1969). *Phys. Lett. B* **30**, 337.
- Hasinoff, M., Fisher, G. A., Kurjan, P., and Hanna, S. S. (1972). *Nucl. Phys. A* **195**, 78.
- Hayward, E., and Fuller, E. G. (1957). *Phys. Rev.* **106**, 991.
- Holt, R. J., and Jackson, H. E. (1975). Argonne National Laboratory Preprint.
- Hotta, A., Itoh, K., and Saito, T. (1974). *Phys. Rev. Lett.* **33**, 790.
- Hughes, T. A., and Fallieros, S. (1969). In 'Nuclear Isospin' (Eds J. D. Anderson, S. D. Bloom, J. Cerny and W. W. True), p. 109 (Academic: New York).
- Jackson, H. E. (1973). Proc. Int. Conf. on Photonuclear Reactions and Applications, Asilomar (Ed. B. L. Berman), Vol. 2, p. 817 (USAEC Office of Information Services: Oak Ridge).

- Klawansky, S., Kendall, H. W., Kerman, A. K., and Isabelle, D. (1973). *Phys. Rev. C* **7**, 795.
- Knöpfle, K. T., Wagner, G. J., Breuer, H., Rogge, M., and Mayer-Böricke, C. (1975). *Phys. Rev. Lett.* **35**, 779.
- Krewald, S., Birkholz, J., Faessler, A., and Speth, J. (1974). Proc. Int. Conf. on Nuclear Structure and Spectroscopy, Amsterdam (Eds H. P. Blok and A. E. L. Dieperink), Vol. 2, p. 111 (Scholar's Press: Amsterdam).
- Kuehne, H. W., Axel, P., and Sutton, D. C. (1967). *Phys. Rev.* **163**, 1278.
- Kuhlmann, E., Ventura, E., Calarco, J. R., Mavis, D. G., and Hanna, S. S. (1975). *Phys. Rev. C* **11**, 1525.
- Kurath, D. (1963). *Phys. Rev.* **130**, 1525.
- Lewis, M. B., and Bertrand, F. E. (1972). *Nucl. Phys. A* **196**, 337.
- Lone, M. A. (1974). Proc. Int. Conf. on Nuclear Structure and Spectroscopy, Amsterdam (Eds H. P. Blok and A. E. L. Dieperink), Vol. 2, p. 314 (Scholar's Press: Amsterdam).
- Marty, N., Morlet, M., Willis, A., Comparat, V., and Frascaria, R. (1975). *Nucl. Phys. A* **238**, 93.
- Maruyama, X. K., Lindgren, R. A., Bendel, W. L., Jones, E. C., Jr, and Fagg, L. W. (1974). *Phys. Rev. C* **10**, 2257.
- Metzger, F. R. (1971). *Nucl. Phys. A* **173**, 141.
- Meyerhof, W. E., Suffert, M., and Feldman, W. (1970). *Nucl. Phys. A* **148**, 211.
- Meyer-Schützmeister, L., Vager, Z., Segel, R. E., and Singh, P. P. (1968). *Nucl. Phys. A* **108**, 180.
- Moalem, A., Benenson, W., and Crawley, G. M. (1973). *Phys. Rev. Lett.* **31**, 482.
- Moalem, A., Benenson, W., and Crawley, G. M. (1974). *Nucl. Phys. A* **236**, 307.
- Moss, J. M., Rozsa, C. M., Youngblood, D. H., Bronson, J. D., and Bacher, A. D. (1975). *Phys. Rev. Lett.* **34**, 748.
- Moss, S. J., and Haerberli, W. (1965). *Nucl. Phys.* **72**, 417.
- Nagao, M., and Torizuka, Y. (1973). *Phys. Rev. Lett.* **30**, 1068.
- Nath, R., Cole, G. W., Firk, F. W. K., Holt, R. J., and Schultz, H. L. (1973). Proc. Int. Conf. on Photonuclear Reactions and Applications, Asilomar (Ed. B. L. Berman), Vol. 1, p. 163 (USAEC Office of Information Services: Oak Ridge).
- O'Connell, W. J. (1969). Ph.D. Thesis, Stanford University.
- O'Connell, W. J., Latshaw, G. L., Black, J. L., and Hanna, S. S. (1973). Proc. Int. Conf. on Photonuclear Reactions and Applications, Asilomar (Ed. B. L. Berman), Vol. 2, p. 939 (USAEC Office of Information Services: Oak Ridge).
- Perrin, G., *et al.* (1974). Proc. Int. Conf. on Nuclear Structure and Spectroscopy, Amsterdam (Eds H. P. Blok and A. E. L. Dieperink), Vol. 1, p. 158 (Scholar's Press: Amsterdam).
- Peschel, R. E., Long, J. M., Shay, H. D., and Bromley, D. A. (1974). *Nucl. Phys. A* **232**, 269.
- Philpott, R. J., and Szydlík, P. P. (1967). *Phys. Rev.* **153**, 1039.
- Pitthan, R. (1973). *Z. Phys.* **260**, 283.
- Pitthan, R., and Walcher, T. (1971). *Phys. Lett. B* **36**, 563.
- Progress Report of the Cyclotron Institute, Texas A&M University (1974).
- Progress Report of the Nuclear Physics Laboratory, Stanford University (1974).
- Riess, F., O'Connell, W. J., Heikkinen, D. W., Kuan, H. M., and Hanna, S. S. (1967). *Phys. Rev. Lett.* **19**, 367.
- Rose, H. J. (1962). *Nucl. Phys.* **128**, 2750.
- Satchler, G. R. (1972). *Nucl. Phys. A* **195**, 1.
- Satchler, G. R. (1973). *Part. Nucl.* **5**, 105.
- Schwierczinski, A., *et al.* (1975). Darmstadt Preprint.
- Shafroth, S. M., and Legge, G. J. F. (1968). *Nucl. Phys. A* **107**, 181.
- Shakin, C. M., and Wang, W. L. (1971). *Phys. Rev. Lett.* **26**, 902.
- Singh, P. P., and Yang, G. C. (1974). Proc. Int. Conf. on Nuclear Structure and Spectroscopy, Amsterdam (Eds H. P. Blok and A. E. L. Dieperink), Vol. 1, p. 162 (Scholar's Press: Amsterdam).
- Smither, R. K., and Bollinger, L. M. (1969). Proc. Int. Symp. on Neutron Capture Gamma-ray Spectroscopy, Studsvik, p. 601 (IAEA: Vienna).
- Snover, K. A., Aldeberger, E. G., and Brown, D. R. (1974a). *Phys. Rev. Lett.* **32**, 1061.
- Snover, K. A., Ebisawa, K., Brown, R. D., and Paul, P. (1974b). *Phys. Rev. Lett.* **32**, 317.
- Spamer, E. (1966). *Z. Phys.* **191**, 24.
- Suffert, M., Feldman, W., Mahieux, J., and Hanna, S. S. (1968). *Nucl. Instrum. Methods* **63**, 1.
- Suzuki, T. (1973). *Nucl. Phys. A* **217**, 182.

- Swann, C. P. (1974). *Phys. Rev. Lett.* **32**, 1449.
- Torizuka, Y., *et al.* (1973). Proc. Int. Conf. on Photonuclear Reactions and Applications, Asilomar (Ed. B. L. Berman) Vol. 1, p. 675 (USAEC Office of Information Services: Oak Ridge).
- Urbas, T. D., and Greiner, W. (1970). *Phys. Rev. Lett.* **24**, 1026.
- Vergados, J. D. (1971). *Phys. Lett. B* **36**, 12.
- Veysseyre, A., Beil, H., Bergère, R., Carlos, P., and Leprêtre, A. (1970). *Nucl. Phys. A* **159**, 561.
- Walcher, T. (1973). Proc. Int. Conf. on Nuclear Physics, Munich (Eds J. de Boer and H. J. Mang), p. 510 (North-Holland: Amsterdam).
- Wang, W. L., and Shakin, C. M. (1973). *Phys. Rev. Lett.* **30**, 301.
- Warburton, E. K., and Pinkston, W. T. (1960). *Phys. Rev.* **118**, 733.
- Watson, R. B., Branford, D., Black, J. L., and Caelli, W. J. (1973). *Nucl. Phys. A* **203**, 209.
- Werntz, C., and Meyerhof, W. E. (1968). *Nucl. Phys. A* **121**, 38.
- Wilkinson, D. H. (1959). *Annu. Rev. Nucl. Sci.* **9**, 1.
- Winhold, E. J., Patrick, B. H., Bowey, E. M., and Gayther, D. B. (1973). Proc. Int. Conf. on Photonuclear Reactions and Applications, Asilomar (Ed. B. L. Berman), Vol. 1, p. 701 (USAEC Office of Information Services: Oak Ridge).
- Young, L. M. (1972). Ph.D. Thesis, University of Illinois.
- Ziegler, J. F., and Peterson, G. A. (1968). *Phys. Rev.* **165**, 1337.

Manuscript received 3 November 1975

